

# SU(2) gauge theory of fluctuating stripe order in the two-dimensional Hubbard model

Henrik Müller-Groeling,<sup>1</sup> Pietro M. Bonetti,<sup>2,1</sup> Paulo Forni,<sup>1</sup> and Walter Metzner<sup>1</sup>

<sup>1</sup>*Max Planck Institute for Solid State Research,  
Heisenbergstrasse 1, D-70569 Stuttgart, Germany*

<sup>2</sup>*Department of Physics, Harvard University, Cambridge MA 02138, USA*

(Dated: March 16, 2026)

We present an SU(2) gauge theory of fluctuating stripe order in the two-dimensional Hubbard model. The theory is based on a fractionalization of the electron operators in fermionic chargons with a pseudospin degree of freedom, and charge neutral spinons capturing fluctuations of the spin orientation. The chargons are treated in a renormalized mean-field theory. We focus on regions of the phase diagram where they undergo stripe order. The spinons are described by a non-linear sigma model with pseudospin stiffnesses determined by the chargons. They prevent breaking of the physical SU(2) spin symmetry at any finite temperature, resulting in a charge ordered pseudogap phase with a reconstructed Fermi surface and a spin gap. The spectral function for single-particle excitations exhibits a collection of Fermi arcs and other structures. The arcs appear in various regions of the Brillouin zone, but never exclusively around the Brillouin zone diagonals.

## I. INTRODUCTION

A universal hallmark of cuprate superconductors – in addition to their high superconducting transition temperatures – is their pseudogap behavior above  $T_c$ , which has been observed in a broad hole-doping range from the underdoped into the optimally doped regime [1]. The pseudogap phenomenology includes several striking properties: a reduction of the charge carrier concentration, a spin gap, and a reconstructed Fermi surface which in photoemission looks like a collection of Fermi arcs. It is often accompanied by electronic nematicity, breaking the tetragonal symmetry of the crystal, and a tendency toward charge order. Suppressing superconductivity by a high magnetic field, the pseudogap regime extends into the other-

wise superconducting region of the phase diagram – for doping concentrations as high as 20 percent [2].

A minimal model describing the strongly correlated valence electrons in the copperoxide planes of cuprate superconductors is the two-dimensional Hubbard model [3, 4]. There is numerical evidence for pseudogap behavior in the two-dimensional Hubbard model, in particular from quantum cluster calculations [5], and a careful analysis of the contributions to the self-energy from effective charge, spin, and pairing interactions has revealed that the pseudogap is generated mainly by antiferromagnetic spin fluctuations [6]. Approximate theories based on quantum field theoretic methods can provide further insight into the structure and mechanisms of the pseudogap behavior, and results for spectroscopic observables with a high energy and momentum resolution. Early theories of the pseudogap phenomenon were based on weak-coupling expansions, such as the Moriya theory [7] and the two-particle self-consistent approach [8]. However, the pseudogap forms only for large magnetic correlation lengths and thus in a narrow parameter regime in these theories, while numerical results show that strong short-ranged correlations are actually sufficient. Alternative previous theories involving only short-range order are based on Anderson’s resonating valence bond (RVB) concept [9], and on dynamical gap generation by umklapp processes [10].

More recently it was shown that the pseudogap behavior observed in cuprates can be captured by SU(2) gauge theories of fluctuating magnetic order [11–17]. This approach is based on a fractionalization of the electron into a fermionic *chargon* with a pseudospin degree of freedom and a charge neutral *spinon*, that is, an SU(2) matrix providing a space and time dependent fluctuating local reference frame [18]. The local spin rotations can be parametrized by an SU(2) gauge field. One can then construct solutions where the chargons exhibit some sort of magnetic order (in particular, Néel, spiral, or stripe), and the Fermi surface gets correspondingly reconstructed. The spinon fluctuations prevent magnetic long-range order of the physical spin-carrying electrons at finite temperatures, and, if strong enough, also in the ground state [19–21]. Quantities involving only charge degrees of freedom behave as in a conventional magnetically ordered state [22–24]. Recently a more sophisticated gauge theory of the pseudogap regime with additional auxiliary degrees of freedom (“ancilla qubits”) was proposed [25–28].

So far, concrete evaluations of SU(2) gauge theories of fluctuating magnetism were restricted to Néel or planar spiral order. In both cases the magnetic order leads to a splitting

of the bare band structure into (only) two quasi-particle bands. In the presence of a sizable next-to-nearest neighbor hopping, as present in the cuprates, Néel order applies to the electron-doped, and spiral order to the lightly hole-doped Hubbard model. However, at larger hole-doping stripe order becomes favorable, at least in mean-field theory [29, 30], and several numerical simulations of the Hubbard model with a sizable hole-doping indicate a stripe-ordered ground state [31–34], sometimes coexisting with superconductivity [35].

In this paper we formulate and evaluate an SU(2) gauge theory of fluctuating stripe order. Our analysis extends the formalism of Ref. [16], which allows for a (approximate) microscopic calculation of observables for interacting electron models. Fluctuating stripe states have also been considered recently in Refs. [36, 37]. The main complication for stripe order, compared to Néel or spiral order, is the large number of quasi-particle bands, which is proportional to the periodicity of the stripe pattern. We solve the chargin sector in a renormalized mean-field theory, and we compute the pseudospin stiffnesses from a renormalized random phase approximation (RPA). The spinon dynamics is governed by a nonlinear sigma model, which is solved in a saddle point approximation. We present results for the quasi-particle Fermi surfaces, the stiffnesses, and the electron spectral function.

The remainder of the article is structured as follows. In Sec. II we describe the general structure of the SU(2) gauge theory of fluctuating stripe order, and our approximate solutions for the chargin and spinon dynamics. Concrete results for the two-dimensional Hubbard model are presented in Sec. III. A conclusion in Sec. IV closes the presentation.

## II. MODEL AND METHOD

While our method could be used for a broader class of models, we consider the Hubbard model on a square lattice [5, 38] for the sake of concreteness. Our calculations are based on the functional integral formalism for quantum many-particle systems [39]. The Hubbard action in imaginary time reads as

$$\begin{aligned} \mathcal{S}[c, c^*] = & \int_0^\beta d\tau \sum_{j,j',\sigma} c_{j\sigma}^* [(\partial_\tau - \mu) \delta_{jj'} + t_{jj'}] c_{j'\sigma} \\ & + \int_0^\beta d\tau U \sum_j n_{j\uparrow} n_{j\downarrow}, \end{aligned} \quad (1)$$

where  $c_{j\sigma} = c_{j\sigma}(\tau)$  and  $c_{j\sigma}^* = c_{j\sigma}^*(\tau)$  are Grassmann fields corresponding to the annihilation and creation, respectively, of an electron with spin orientation  $\sigma$  at site  $j$ , and  $n_{j\sigma} = n_{j\sigma}(\tau) = c_{j\sigma}^*(\tau)c_{j\sigma}(\tau)$ . The hopping amplitudes  $t_{jj'}$  are translation invariant, that is, they depend only on  $j - j'$ . The chemical potential is denoted by  $\mu$ , and  $U > 0$  is the strength of the (repulsive) Hubbard interaction. To simplify the notation, we write the dependence of the fields on the imaginary time  $\tau$  only if needed for clarity. The Hubbard action in (1) is invariant under *global* SU(2) spin rotations  $c_j(\tau) \rightarrow \mathcal{U}c_j(\tau)$ ,  $c_j^*(\tau) \rightarrow c_j^*(\tau)\mathcal{U}^\dagger$ , where  $c_j$  and  $c_j^*$  are two-component spinors composed from  $c_{j\sigma}$  and  $c_{j\sigma}^*$  with  $\sigma \in \{\uparrow, \downarrow\}$ , respectively, while  $\mathcal{U}$  is an arbitrary SU(2) matrix.

### A. Electron fractionalization

To separate spin orientation fluctuations from the charge degrees of freedom, we fractionalize the electronic fields as [18–21]

$$c_j(\tau) = R_j(\tau) \psi_j(\tau), \quad c_j^*(\tau) = \psi_j^*(\tau) R_j^\dagger(\tau), \quad (2)$$

where  $R_j(\tau) \in \text{SU}(2)$ , to which we refer as *spinon*, is composed of bosonic fields, and the components  $\psi_{js}$  of the *chargon* spinor  $\psi_j$  are fermionic. The spinons transform under the global SU(2) spin rotation by a *left* matrix multiplication, while the chargons are left invariant. Conversely, a U(1) charge transformation acts only on  $\psi_j$ , leaving  $R_j$  unaffected. The factorization in Eq. (2) introduces a redundant *local* SU(2) symmetry, acting as

$$\psi_j(\tau) \rightarrow \mathcal{V}_j(\tau) \psi_j(\tau), \quad \psi_j^*(\tau) \rightarrow \psi_j^*(\tau) \mathcal{V}_j^\dagger(\tau), \quad (3a)$$

$$R_j(\tau) \rightarrow R_j(\tau) \mathcal{V}_j^\dagger(\tau), \quad R_j^\dagger(\tau) \rightarrow \mathcal{V}_j(\tau) R_j^\dagger(\tau), \quad (3b)$$

with  $\mathcal{V}_j \in \text{SU}(2)$ . Hence, the components  $\psi_{js}$  of  $\psi_j$  carry an SU(2) gauge index  $s$ , while the components  $R_{j,\sigma s}$  of  $R_j$  have two indices, the first one ( $\sigma$ ) corresponding to the global SU(2) symmetry, and the second one ( $s$ ) to SU(2) gauge transformations.

We now rewrite the Hubbard action in terms of the spinon and chargon fields. The quadratic part of (1) can be expressed as [20]

$$\begin{aligned} \mathcal{S}_0[\psi, \psi^*, R] = & \int_0^\beta d\tau \left\{ \sum_j \psi_j^* [\partial_\tau - \mu - \phi_j] \psi_j \right. \\ & \left. + \sum_{j,j'} t_{jj'} \psi_j^* e^{iA_{jj'}} \psi_{j'} \right\}, \end{aligned} \quad (4)$$

where we have introduced a fictitious SU(2) gauge field, defined by

$$\begin{aligned}\phi_j(\tau) &= -R_j^\dagger(\tau)\partial_\tau R_j(\tau), \\ e^{iA_{jj'}(\tau)} &= R_j^\dagger(\tau)R_{j'}(\tau).\end{aligned}\tag{5}$$

Both  $\phi_j(\tau)$  and  $A_{jj'}(\tau)$  are elements of the Lie algebra of SU(2), and can therefore be written as linear combinations of the Pauli matrices  $\sigma^1$ ,  $\sigma^2$ , and  $\sigma^3$ :

$$\begin{aligned}\phi_j(\tau) &= \frac{1}{2} \sum_a \phi_j^a(\tau) \sigma^a, \\ A_{jj'}(\tau) &= \frac{1}{2} \sum_a A_{jj'}^a(\tau) \sigma^a.\end{aligned}\tag{6}$$

$A_{jj'}(\tau)$  contributes to the action only if the sites  $j$  and  $j'$  are coupled by a hopping amplitude.

In the interaction part of the Hubbard action (1), the SU(2) rotations drop out [16], so that

$$\mathcal{S}_{\text{int}}[\psi, \psi^*, R] = \mathcal{S}_{\text{int}}[\psi, \psi^*] = \int_0^\beta d\tau U \sum_j n_{j\uparrow}^\psi n_{j\downarrow}^\psi,\tag{7}$$

with  $n_{j_s}^\psi = \psi_{j_s}^* \psi_{j_s}$ . The action  $\mathcal{S} = \mathcal{S}_0 + \mathcal{S}_{\text{int}}$  is nothing but the Hubbard model action where the physical electrons have been replaced by chargons coupled to an SU(2) gauge field.

## B. Spinon effective action

We now derive an effective action for the spinon fields. Assigning only long wave length spin orientation fluctuations to the rotation matrices  $R_j(\tau)$ , we can assume that  $R_j(\tau)$  is slowly varying in space. Under this assumption, the gauge fields  $A_{jj'}^a(\tau)$  can be linearized as

$$A_{jj'}^a(\tau) = \mathbf{r}_{jj'} \cdot \mathbf{A}_j^a(\tau) = x_{jj'} A_{x,j}^a(\tau) + y_{jj'} A_{y,j}^a(\tau),\tag{8}$$

where  $\mathbf{r}_{jj'} = \mathbf{r}_j - \mathbf{r}_{j'}$  is the real space vector from site  $j'$  to site  $j$ , while  $x_{jj'}$  and  $y_{jj'}$  are its  $x$  and  $y$  components, respectively. The spatial components of the gauge field  $A_{\alpha,j}^a$  with  $\alpha = x, y$  can be combined with the temporal components  $A_{0,j}^a \equiv \phi_j^a$  to a 3-vector  $A_{\mu,j}^a$  with  $\mu = 0, x, y$ .

For slowly varying rotation matrices  $R_j(\tau)$ , an expansion in the gauge fields corresponds to a gradient expansion. We will carry out this expansion to quadratic order. Hence, we derive the effective action for the spinons from an expansion of  $\mathcal{S}_0[\psi, \psi^*, A]$  in Eq. (4) to

quadratic order in  $A$ . Fourier transforming  $\psi_j(\tau)$  to  $\psi(k)$  with  $k = (\mathbf{k}, ik_0) = (k_x, k_y, ik_0)$ , and  $A_{\mu,j}^a(\tau)$  to  $A_\mu^a(q)$  with  $q = (\mathbf{q}, iq_0) = (q_x, q_y, iq_0)$ , one obtains [40]

$$\begin{aligned} \mathcal{S}_0[\psi, \psi^*, A] = & - \int_k \psi^*(k) (ik_0 + \mu - \epsilon_{\mathbf{k}}) \psi(k) \\ & - \frac{1}{2} \int_{k,q} \sum_a A_\mu^a(q) \gamma_{\mathbf{k}}^\mu \psi^*(k+q) \sigma^a \psi(k) \\ & + \frac{1}{8} \int_{k,q,q'} \sum_a A_\alpha^a(q-q') A_\beta^a(q') \gamma_{\mathbf{k}}^{\alpha\beta} \psi^*(k+q) \psi(k), \end{aligned} \quad (9)$$

with the first and second order coupling functions  $\gamma_{\mathbf{k}}^\mu = (1, \nabla_{\mathbf{k}} \epsilon_{\mathbf{k}})$  and  $\gamma_{\mathbf{k}}^{\alpha\beta} = \partial_{k_\alpha k_\beta}^2 \epsilon_{\mathbf{k}}$ , respectively, and  $\epsilon_{\mathbf{k}}$  is the Fourier transform of the hopping amplitudes  $t_{jj'}$ . Here and in the following equations, we use Einstein's summation convention for repeated space-time indices, while sums over spin indices are written explicitly. The integrals are written in a shorthand notation  $\int_k = T \sum_{k_0} \int \frac{d^2 \mathbf{k}}{(2\pi)^2}$ , and analogously for  $\int_q$ , where  $k_0$  and  $q_0$  are fermionic and bosonic Matsubara frequencies, respectively.

Integrating out the fermionic fields from the action  $\mathcal{S}[\psi, \psi^*, A] = \mathcal{S}_0[\psi, \psi^*, A] + \mathcal{S}_{\text{int}}[\psi, \psi^*]$ , one obtains an effective action  $\mathcal{S}[A]$  for the gauge fields. For slowly varying fluctuations, we can expand this action in powers of  $A$ . The linear term vanishes [16] except for a Berry term [20] which is probably irrelevant [41]. The quadratic term has the form

$$\mathcal{S}[A] = \frac{1}{2} \int_{q,q'} \sum_{a,b} K_{\mu\nu}^{ab}(q, q') A_\mu^a(q) A_\nu^b(-q'), \quad (10)$$

with a function  $K_{\mu\nu}^{ab}$  we refer to as ‘‘gauge kernel’’ in the following. While the frequencies  $q_0$  and  $q'_0$  contributing to Eq. (10) are always equal, the momenta  $\mathbf{q}$  and  $\mathbf{q}'$  can differ by reciprocal lattice vectors of the magnetic state, which breaks the translation invariance. If  $\mathbf{q}$  and  $\mathbf{q}'$  are so small that  $\mathbf{q} - \mathbf{q}'$  is smaller than any non-zero reciprocal lattice vector, one can assume that  $\mathbf{q} = \mathbf{q}'$ , and Eq. (10) simplifies to

$$\mathcal{S}[A] = \frac{1}{2} \int_q \sum_{a,b} K_{\mu\nu}^{ab}(q) A_\mu^a(q) A_\nu^b(-q). \quad (11)$$

In the following we will consider only the contributions from  $\mathbf{q} = \mathbf{q}'$ . The gauge kernel is a sum of a *paramagnetic* and a *diamagnetic* contribution,  $K_{\mu\nu}^{ab} = K_{\mu\nu}^{p,ab} + K_{\mu\nu}^{d,ab}$ , where

$$K_{\mu\nu}^{p,ab}(q) = -\frac{1}{4} \int_{k,k'} \gamma_{\mathbf{k}}^\mu \gamma_{\mathbf{k}'}^\nu \langle \psi^*(k-q) \sigma^a \psi(k) \psi^*(k'+q) \sigma^b \psi(k') \rangle, \quad (12a)$$

$$K_{\mu\nu}^{d,ab} = \frac{1}{4} \delta_{ab} \delta_{\mu\alpha} \delta_{\nu\beta} \int_k \gamma_{\mathbf{k}}^{\alpha\beta} \langle \psi^*(k) \psi(k) \rangle. \quad (12b)$$

The brackets  $\langle \dots \rangle$  are connected expectation values for chargons in the absence of the gauge field  $A$ , but in the presence of an infinitesimal  $SU(2)$  symmetry breaking external field  $h$ , whose role and precise form will be described later. The diamagnetic term is momentum and frequency independent, and contributes only if  $\mu$  and  $\nu$  are both spatial indices  $\alpha, \beta \in \{x, y\}$ .

In this work we approximate the gauge kernel  $K_{\mu\nu}^{ab}(q)$  in the effective action  $\mathcal{S}[A]$  by its low energy and long wavelength limit  $q \rightarrow 0$ . More specifically, its spatial components  $K_{\alpha\beta}^{ab}(q)$  with  $\alpha, \beta \in \{x, y\}$  are approximated by the *spatial spin stiffness*

$$J_{\alpha\beta}^{ab} = \lim_{h \rightarrow 0} \lim_{\mathbf{q} \rightarrow \mathbf{0}} K_{\alpha\beta}^{ab}(\mathbf{q}, 0), \quad (13)$$

and its temporal component  $K_{00}^{ab}(q)$  is approximated by the *temporal spin stiffness*

$$Z^{ab} = -J_{00}^{ab} = -\lim_{h \rightarrow 0} \lim_{q_0 \rightarrow 0} K_{00}^{ab}(\mathbf{0}, iq_0). \quad (14)$$

The discrete set of Matsubara frequencies at finite temperature has been continued to the entire imaginary frequency axis to take the limit  $q_0 \rightarrow 0$ . Alternatively one may analytically continue  $q_0$  to the real frequency axis, and then take the zero frequency limit along that axis. The limits  $\mathbf{q} \rightarrow \mathbf{0}$ ,  $q_0 \rightarrow 0$ , and  $h \rightarrow 0$  do not commute. Their order must therefore be specified. We neglect the mixed spatio-temporal components  $J_{\alpha 0}^{ab}$  and  $J_{0\beta}^{ab}$ . They are imaginary and due to Landau damping.

The action in Eq. (11) can then be written as a *local* action in a real space continuum representation,

$$\mathcal{S}[A] = \frac{1}{2} \int dx \sum_{a,b} J_{\mu\nu}^{ab} A_\mu^a(x) A_\nu^b(x), \quad (15)$$

where  $x = (\mathbf{r}, -i\tau)$  and  $A_\mu^a(x)$  is the Fourier transform of  $A_\mu^a(q)$ . This form of the effective action has already been used in the case of spiral magnetic order in [16]. The action (15) can be mapped to a nonlinear sigma model of the form [16]

$$\mathcal{S}[\mathcal{R}] = \frac{1}{2} \int dx \text{tr} \{ \mathcal{P}_{\mu\nu} [\partial_\mu \mathcal{R}^T(x)] [\partial_\nu \mathcal{R}(x)] \}, \quad (16)$$

where  $\mathcal{R}$  is the adjoint representation of the  $SU(2)$  rotation  $R$ , defined by

$$R^\dagger \sigma^a R = \sum_b \mathcal{R}^{ab} \sigma^b, \quad (17)$$

and  $\partial_\mu = (\nabla, i\partial_\tau)$ . The coefficients are given by  $\mathcal{P}_{\mu\nu} = \frac{1}{2} \text{tr}(\mathcal{J}_{\mu\nu}) \mathbb{1} - \mathcal{J}_{\mu\nu}$ , where  $\mathcal{J}_{\mu\nu}$  is the  $3 \times 3$  stiffness matrix with matrix elements  $J_{\mu\nu}^{ab}$ .

## C. Chargons

### 1. Renormalized mean-field theory

We deal with the chargons in a renormalized mean-field theory as formulated in Ref. [42]. Mean-field equations for ordered phases are thereby solved with renormalized instead of bare interactions as input parameters. The renormalized interactions are obtained from a functional renormalization group flow [43], which takes charge, spin, and pairing channels into account on equal footing. This approach has been applied to the Hubbard model in several papers [16, 44, 45]. The coupled fluctuations of the various channels have two important effects: i) magnetic interactions are reduced, and ii) d-wave pairing interactions are generated by fluctuations [43]. Since we are interested in the normal (non-superconducting) state, we ignore the pairing instability by assuming that the temperature is above the transition temperature for pairing, or that superconductivity has been suppressed by an external magnetic field.

The effective interactions are momentum and frequency dependent, but these dependences are rather weak for the *two-particle irreducible* [42] effective interactions which enter the mean-field equations. Hence we compute the effective interaction in the magnetic channel at zero frequency and at the wave vector  $\mathbf{Q}$  where the magnetic interaction is maximal, and use this as a momentum and frequency independent coupling constant  $\bar{U}$ . Using the most general mean-field (Hartree-Fock) decoupling of the effective interaction in the charge and spin channels [29, 46], one then obtains the renormalized mean-field interaction

$$\begin{aligned}
 H_{\text{MF}}^I = & \sum_j \left[ \Delta_j^c \psi_j^\dagger \sigma^0 \psi_j - \bar{U}^{-1} (\Delta_j^c)^2 \right] \\
 & - \sum_j \sum_{a=1}^3 \left[ \Delta_j^a \psi_j^\dagger \sigma^a \psi_j - \bar{U}^{-1} (\Delta_j^a)^2 \right],
 \end{aligned}
 \tag{18}$$

where  $\psi_j$  is the two-component spinor composed of the annihilation operators  $\psi_{j\uparrow}$  and  $\psi_{j\downarrow}$ , and  $\psi_j^\dagger$  is its hermitian conjugate;  $\sigma^0$  is the two-dimensional identity matrix and  $\sigma^1, \sigma^2, \sigma^3$  are the Pauli matrices.

## 2. Stripe order

In a sizable parameter range, the energetically most favorable solution of the (renormalized) mean-field equations yields collinear spin order accompanied by charge order, also known as spin-charge stripe order [29, 46–51]. In the following we focus our analysis on this stripe-ordered regime. The direction of the collinear spin order can be chosen arbitrarily. Assuming an orientation of the spins in  $x$ -direction, the order parameters  $\Delta_j^2$  and  $\Delta_j^3$  in Eq. (18) vanish, and we are left with  $\Delta_j^c$  and  $\Delta_j^s \equiv \Delta_j^1$  defined by the expectation values

$$\Delta_j^c = \frac{1}{2} \bar{U} \langle \psi_j^\dagger \sigma^0 \psi_j \rangle = \frac{1}{2} \bar{U} \rho_j, \quad (19a)$$

$$\Delta_j^s = \frac{1}{2} \bar{U} \langle \psi_j^\dagger \sigma^1 \psi_j \rangle = \bar{U} m_j^1, \quad (19b)$$

where  $\rho_j$  is the local charge density, and  $m_j^1$  the local spin density in  $x$ -direction. Except for a restricted region near the edge of the magnetically ordered regime (at fairly large doping), the stripe order is usually *unidirectional*, that is, along one of the axes of the square lattice spins order perfectly antiferromagnetically, while the charge density is uniform along that axis [29, 30]. Assuming an antiferromagnetic alignment (and uniform charge density) in the  $y$ -direction, the wave vectors describing the stripe order in Fourier space have the form  $\mathbf{Q} = (\pi - 2\pi\eta, \pi)$ , where  $\eta$  parametrizes the deviation from Néel order in  $x$ -direction.

For concrete calculations we assume that the stripe order is commensurate with a period  $p$ , that is, the ordering pattern is invariant under translations by  $p$  lattice sites in  $x$ -direction. Incommensurate wave vectors can be approximated to any desired accuracy by commensurate wave vectors with sufficiently large periods  $p$ . The spin and charge profile can then be expanded in a finite Fourier series [30]

$$m_j^1 = \sum_{n \text{ odd}} M_n e^{i\mathbf{Q}_n \cdot \mathbf{r}_j}, \quad (20a)$$

$$\rho_j = \sum_{n \text{ even}} \varrho_n e^{i\mathbf{Q}_n \cdot \mathbf{r}_j}, \quad (20b)$$

where  $\mathbf{Q}_n = (2\pi n/p, \pi n)$ , and  $\mathbf{r}_j$  are the coordinates of the lattice site  $j$ . The indices  $n$  are integer numbers from  $\{0, 1, \dots, P-1\}$ , where  $P$  is the smallest positive integer satisfying  $P\mathbf{Q}_1 = (0, 0)$  modulo reciprocal lattice vectors. Hence,  $P = p$  if  $p$  is even, and  $P = 2p$  if  $p$  is odd. The first sum is running only over odd integers because the spin order is antiferromagnetic in  $y$ -direction, while the second sum is restricted to even integers since  $\rho_j$

is translation invariant in  $y$ -direction. The order parameters in Eq. (19) can be expanded accordingly

$$\Delta_j^s = \sum_{n \text{ odd}} \Delta_n^s e^{i\mathbf{Q}_n \cdot \mathbf{r}_j}, \quad (21a)$$

$$\Delta_j^c = \sum_{n \text{ even}} \Delta_n^c e^{i\mathbf{Q}_n \cdot \mathbf{r}_j}, \quad (21b)$$

with  $\Delta_n^c = \frac{1}{2}\bar{U}\varrho_n$  and  $\Delta_n^s = \bar{U}M_n$ . Since  $\Delta_j^c$  and  $\Delta_j^s$  are real numbers, their Fourier components obey the relations  $\Delta_n^c = (\Delta_{P-n}^c)^*$  and  $\Delta_n^s = (\Delta_{P-n}^s)^*$ .

Inserting Eq. (21) into Eq. (18), and Fourier transforming, yields the mean-field Hamiltonian in momentum representation,

$$\begin{aligned} H_{\text{MF}} = & \int_{\mathbf{k}} \epsilon_{\mathbf{k}} \psi_{\mathbf{k}}^\dagger \psi_{\mathbf{k}} \\ & + \int_{\mathbf{k}} \sum_{n=0}^{P-1} \left( \Delta_n^c \psi_{\mathbf{k}}^\dagger \sigma^0 \psi_{\mathbf{k}+\mathbf{Q}_n} - \Delta_n^s \psi_{\mathbf{k}}^\dagger \sigma^1 \psi_{\mathbf{k}+\mathbf{Q}_n} \right) \\ & - \sum_{n=0}^{P-1} \left( \bar{U}^{-1} |\Delta_n^c|^2 - \bar{U}^{-1} |\Delta_n^s|^2 \right), \end{aligned} \quad (22)$$

where  $\Delta_n^c = 0$  for odd  $n$  and  $\Delta_n^s = 0$  for even  $n$ . Absorbing  $\Delta_0^c$  into the chemical potential we can also set  $\Delta_0^c = 0$ .

Introducing a "Nambu spinor" with  $P$  components

$$\Psi_{\mathbf{k},\sigma} = \begin{pmatrix} \psi_{\mathbf{k},\sigma} \\ \psi_{\mathbf{k}+\mathbf{Q}_1,\bar{\sigma}} \\ \psi_{\mathbf{k}+\mathbf{Q}_2,\sigma} \\ \vdots \\ \psi_{\mathbf{k}+\mathbf{Q}_{P-2},\sigma} \\ \psi_{\mathbf{k}+\mathbf{Q}_{P-1},\bar{\sigma}} \end{pmatrix}, \quad (23)$$

with the convention  $\bar{\uparrow} = \downarrow$  and  $\bar{\downarrow} = \uparrow$ , one can cast the Hamiltonian (22) in the form

$$H_{\text{MF}} = \sum_{\sigma} \int'_{\mathbf{k}} \Psi_{\mathbf{k},\sigma}^\dagger \mathcal{H}_{\mathbf{k}} \Psi_{\mathbf{k},\sigma}, \quad (24)$$

where we have dropped the constant term in Eq. (22). The momentum integration  $\int'_{\mathbf{k}} = \int_{\mathbf{k} \in \text{BZ}'} \frac{d^2\mathbf{k}}{(2\pi)^2}$ , extends over a reduced Brillouin zone BZ' corresponding to the reduced translation invariance in the stripe ordered state [30]. The matrix  $\mathcal{H}_{\mathbf{k}}$  has  $P \times P$  elements of the

form

$$[\mathcal{H}_{\mathbf{k}}]_{ll'} = \begin{cases} \epsilon_{\mathbf{k}+\mathbf{Q}_l} & \text{if } l = l' \\ -\Delta_n^s & \text{if } l' = (l+n) \bmod P, n \text{ odd} \\ \Delta_n^c & \text{if } l' = (l+n) \bmod P, n \text{ even} \end{cases} . \quad (25)$$

For example, for  $P = 6$ , we have

$$\mathcal{H}_{\mathbf{k}} = \begin{pmatrix} \epsilon_{\mathbf{k}} & -\Delta_1^s & \Delta_2^c & -\Delta_3^s & \Delta_4^c & -\Delta_5^s \\ -\Delta_5^s & \epsilon_{\mathbf{k},1} & -\Delta_1^s & \Delta_2^c & -\Delta_3^s & \Delta_4^c \\ \Delta_4^c & -\Delta_5^s & \epsilon_{\mathbf{k},2} & -\Delta_1^s & \Delta_2^c & -\Delta_3^s \\ -\Delta_3^s & \Delta_4^c & -\Delta_5^s & \epsilon_{\mathbf{k},3} & -\Delta_1^s & \Delta_2^c \\ \Delta_2^c & -\Delta_3^s & \Delta_4^c & -\Delta_5^s & \epsilon_{\mathbf{k},4} & -\Delta_1^s \\ -\Delta_1^s & \Delta_2^c & -\Delta_3^s & \Delta_4^c & -\Delta_5^s & \epsilon_{\mathbf{k},5} \end{pmatrix}, \quad (26)$$

where  $\epsilon_{\mathbf{k},l} = \epsilon_{\mathbf{k}+\mathbf{Q}_l}$ .

The matrix  $\mathcal{H}_{\mathbf{k}}$  can be diagonalized by a unitary transformation  $\mathcal{U}_{\mathbf{k}}$ . The corresponding eigenvalues  $E_{\mathbf{k}}^\ell$  with  $\ell = 1, \dots, P$  describe the quasi-particle bands of the stripe state. The mean-field free energy is thus given by

$$F = -2T \int_{\mathbf{k}} \sum_{\ell=1}^P \ln \left( 1 + e^{-E_{\mathbf{k}}^\ell/T} \right) - \sum_{n=0}^{P-1} (\bar{U}^{-1} |\Delta_n^c|^2 - \bar{U}^{-1} |\Delta_n^s|^2) + \mu n, \quad (27)$$

where the chemical potential  $\mu$  is determined by adjusting the density  $n = 2 \int_{\mathbf{k}} \sum_{\ell} f(E_{\mathbf{k}}^\ell)$  to a given value.

### 3. Chargon Green function

The chargon Green function is defined as the expectation value

$$G_{\sigma\sigma'}(k, k') = -\langle \psi_{\sigma}(k) \psi_{\sigma'}^*(k') \rangle. \quad (28)$$

$G_{\sigma\sigma}(k, k')$  is non-zero only for  $k_0 = k'_0$  and  $\mathbf{k} = \mathbf{k}' + \mathbf{Q}_n$  with even  $n$ , while  $G_{\sigma\bar{\sigma}}(k, k')$  is non-zero only for  $k_0 = k'_0$  and  $\mathbf{k} = \mathbf{k}' + \mathbf{Q}_n$  with odd  $n$ . Using the Grassmann field  $\Psi_{\sigma}(k)$  corresponding to the Nambu spinor  $\Psi_{\mathbf{k}\sigma}$  defined in Eq. (23), the non-zero contributions to  $G_{\sigma\sigma'}(k, k')$  can be conveniently collected in a matrix Green function

$$\mathcal{G}_{\sigma}(k) = -\langle \Psi_{\sigma}(k) \Psi_{\sigma}^*(k) \rangle = (ik_0 - \mathcal{H}_{\mathbf{k}})^{-1}. \quad (29)$$

Note that  $\mathcal{G}_\uparrow = \mathcal{G}_\downarrow$  since  $\mathcal{H}_\mathbf{k}$  is independent of  $\sigma$ . This is equivalent to the relations  $G_{\uparrow\uparrow}(k, k') = G_{\downarrow\downarrow}(k, k')$  and  $G_{\uparrow\downarrow}(k, k') = G_{\downarrow\uparrow}(k, k')$ . From  $\mathcal{U}_\mathbf{k}^\dagger \mathcal{H}_\mathbf{k} \mathcal{U}_\mathbf{k} = \text{diag}(E_\mathbf{k}^1, \dots, E_\mathbf{k}^P)$  we obtain  $\mathcal{U}_\mathbf{k}^\dagger \mathcal{G}_\sigma(k) \mathcal{U}_\mathbf{k} = \text{diag}[(ik_0 - E_\mathbf{k}^1)^{-1}, \dots, (ik_0 - E_\mathbf{k}^P)^{-1}]$ , and thus

$$\mathcal{G}_\sigma(k) = \sum_\ell \frac{g_\mathbf{k}^\ell}{ik_0 - E_\mathbf{k}^\ell}, \quad (30)$$

where  $g_\mathbf{k}^\ell$  is the  $P \times P$  matrix formed from the elements  $(g_\mathbf{k}^\ell)_{ll'} = (\mathcal{U}_\mathbf{k})_{l\ell} (\mathcal{U}_\mathbf{k}^\dagger)_{\ell'l}$ .

Using the definition of the charge and magnetic gaps Eq. (19), and their Fourier expansion Eq. (21), one can write their self-consistency equations in terms of the Green function as

$$\Delta_n^c = -\bar{U} \int_k \langle \psi_\sigma(k + Q_n) \psi_\sigma^*(k) \rangle = \bar{U} \int_k G_{\sigma\sigma}(k + Q_n, k), \quad (31a)$$

$$\Delta_n^s = -\bar{U} \int_k \langle \psi_{\bar{\sigma}}(k + Q_n) \psi_\sigma^*(k) \rangle = \bar{U} \int_k G_{\bar{\sigma}\sigma}(k + Q_n, k), \quad (31b)$$

where  $Q_n = (0, \mathbf{Q}_n)$ . Using the spectral decomposition Eq. (30), the Matsubara summation on the right hand sides of these gap equations can be performed analytically.

#### 4. Chargon susceptibility

The dynamical spin susceptibility of the chargons is defined as the connected expectation value

$$\chi^{ab}(x, x') = \langle S_\psi^a(x) S_\psi^b(x') \rangle_c, \quad (32)$$

where the variable  $x = (\mathbf{r}, -i\tau)$  comprises the imaginary time  $\tau$  and the lattice vectors  $\mathbf{r} = \mathbf{r}_j$ , while  $S_\psi^a(x) = \frac{1}{2} \psi^*(x) \sigma^a \psi(x)$  is the chargon pseudospin field expressed as a bilinear form of the chargon fields.

#### D. Ward identity

In this section we derive a Ward identity relating the gauge kernel  $K_{\mu\nu}^{ab}$  to the spin susceptibility  $\chi^{ab}$  in the stripe ordered state. This identity shows that the spin stiffness obtained from the gauge kernel is equivalent to a stiffness defined via the spin susceptibility. Similar Ward identities have already been obtained for Néel and spiral order [40, 52, 53]. In this section, we use a summation convention also for repeated spin indices.

The Ward identity involves a static symmetry breaking external field  $\mathbf{h}(\mathbf{r})$  coupled linearly to the spin field  $\mathbf{S}(x)$ . We choose this field to have the same spatial form as the expectation value of  $\mathbf{S}(x)$  in the ordered state,

$$\mathbf{h}(\mathbf{r}) = \frac{h}{m} \mathbf{m}(\mathbf{r}) = \frac{h}{m} \langle \mathbf{S}(x) \rangle, \quad (33)$$

where  $h$  parametrizes the amplitude of the external field, and  $m$  is the amplitude of the order parameter defined as

$$m^2 = L^{-1} \sum_{\mathbf{r}} [\mathbf{m}(\mathbf{r})]^2 = P^{-1} \sum_{\bar{\mathbf{r}}} [\mathbf{m}(\bar{\mathbf{r}})]^2, \quad (34)$$

where  $L$  is the number of lattice sites, and the sum over  $\bar{\mathbf{r}}$  is restricted to one unit cell (containing  $P$  lattice sites). Note that  $\langle \mathbf{S}(x) \rangle$  does not depend on time.

From global SU(2) symmetry one can derive the following identity [52]

$$\int_{x,x'} \epsilon^{abc} \epsilon^{a'b'c'} \chi^{bb'}(x, x') h^c(\mathbf{r}) h^{c'}(\mathbf{r}') = \frac{m}{h} \int_x (\delta_{aa'} \delta_{cc'} - \delta_{ac} \delta_{a'c'}) h^c(\mathbf{r}) h^{c'}(\mathbf{r}'), \quad (35)$$

which is valid for any magnetic order. Specifying stripe order with all spins (and thus  $h^a(\mathbf{r})$ ) aligned in  $x$ -direction, this relation simplifies to

$$\int_{x,x'} \chi^{aa'}(x, x') h^1(\mathbf{r}) h^1(\mathbf{r}') = \begin{cases} \frac{m}{h} \int_x [h^1(\mathbf{r})]^2 & \text{for } a = a' \in \{2, 3\} \\ 0 & \text{else} \end{cases}. \quad (36)$$

We define a *weighted* spin correlation function as

$$\tilde{\chi}^{aa'}(x, x') = \frac{1}{m^2} m^1(\mathbf{r}) m^1(\mathbf{r}') \chi^{aa'}(x, x'), \quad (37)$$

and denote its Fourier transform by  $\tilde{\chi}^{ab}(q, q')$ . Substituting  $h^1(\mathbf{r})$  by  $S^1(\mathbf{r})$  and using Eq. (34), Eq. (36) can then be expressed as

$$\tilde{\chi}^{aa'}(q, q') \Big|_{q=q'=0} = \begin{cases} m/h & \text{for } a = a' \in \{2, 3\} \\ 0 & \text{else} \end{cases}. \quad (38)$$

From local SU(2) symmetry one can derive the Ward identity [52]

$$\begin{aligned} \partial_\mu \partial'_\nu K_{\mu\nu}^{aa'}(x, x') &= -\epsilon^{abc} \epsilon^{a'b'c'} \chi^{bb'}(x, x') h^c(\mathbf{r}) h^{c'}(\mathbf{r}') \\ &\quad - (2\delta_{ac} \delta_{a'c'} - \delta_{ac'} \delta_{a'c} - \delta_{aa'} \delta_{cc'}) m^c(\mathbf{r}) h^{c'}(\mathbf{r}') \delta(x - x'). \end{aligned} \quad (39)$$

The continuum limit for the spatial derivatives is legitimate here because we will evaluate the Ward identity in Fourier space for small momenta only. For stripe order with all spins aligned in  $x$ -direction, this yields

$$\partial_\mu \partial'_\nu K_{\mu\nu}^{aa'}(x, x') = \begin{cases} -\chi^{\bar{a}\bar{a}}(x, x') h^1(\mathbf{r}) h^1(\mathbf{r}') + m^1(\mathbf{r}) h^1(\mathbf{r}) \delta(x - x') & \text{for } a = a' \in \{2, 3\} \\ \chi^{\bar{a}\bar{a}'}(x, x') h^1(\mathbf{r}) h^1(\mathbf{r}') & \text{for } a \neq a' \in \{2, 3\} \\ 0 & \text{else} \end{cases} , \quad (40)$$

where  $\bar{2} = 3$  and  $\bar{3} = 2$ . Substituting  $h^1(\mathbf{r})$  by  $m^1(\mathbf{r})$  and Fourier transforming, one obtains

$$(\mathbf{q}, iq_0)_\mu (\mathbf{q}', iq'_0)_\nu K_{\mu\nu}^{aa'}(q, q') = \begin{cases} -h^2 \tilde{\chi}^{\bar{a}\bar{a}}(q, q') + hm & \text{for } a = a' \in \{2, 3\} \\ h^2 \tilde{\chi}^{\bar{a}\bar{a}'}(q, q') & \text{for } a \neq a' \in \{2, 3\} \\ 0 & \text{else} \end{cases} . \quad (41)$$

Eq. (38) then implies

$$(\mathbf{q}, iq_0)_\mu (\mathbf{q}', iq'_0)_\nu K_{\mu\nu}^{aa'}(q, q') \Big|_{q=q'=0} = 0 , \quad (42)$$

for all  $a, a'$ .

Taking second derivatives with respect to momenta and frequencies, the Ward identity Eq. (41) relates the spatial and temporal stiffnesses defined in Eqs. (13) and (14), respectively, to the weighted susceptibility  $\tilde{\chi}^{aa}$ . In particular,  $J_{\mu\nu}^{a1} = J_{\mu\nu}^{1a} = 0$  for all  $a$ , while

$$J_{\alpha\beta}^{aa} = -\frac{1}{2} \lim_{h \rightarrow 0} h^2 \partial_{q_\alpha} \partial_{q_\beta} \tilde{\chi}^{\bar{a}\bar{a}}(q, q) \Big|_{q=0} , \quad (43)$$

$$Z^{aa} = -\frac{1}{2} \lim_{h \rightarrow 0} h^2 \partial_{q_0}^2 \tilde{\chi}^{\bar{a}\bar{a}}(q, q) \Big|_{q=0} , \quad (44)$$

for  $a \in \{2, 3\}$  and  $\alpha, \beta \in \{x, y\}$ . In the special case of Néel order one has  $m^1(\mathbf{r}) = m e^{i\mathbf{Q}\mathbf{r}}$  with  $\mathbf{Q} = (\pi, \pi)$ , so that  $\tilde{\chi}^{ab}(q, q) = \chi^{ab}(Q + q, Q + q)$  with  $Q = (\mathbf{Q}, 0)$ . The relations (43) and (44) then agree with those derived in Refs. [52, 53]. It is crucial to take the limit  $h \rightarrow 0$  *after* the limit  $q \rightarrow 0$ . Taking the limits in the opposite order would yield  $J_{\mu\nu}^{aa'} = 0$  for all  $a, a'$ .

The equivalence of the  $y$  and  $z$  directions for a stripe state with all spins aligned in  $x$ -direction implies that  $\chi^{22} = \chi^{33} \equiv \chi^\perp$ , so that  $J_{\alpha\beta}^{22} = J_{\alpha\beta}^{33} \equiv J_{\alpha\beta}$  and  $Z^{22} = Z^{33} \equiv Z$ . Eqs. (38), (43), and (44) are consistent with

$$\tilde{\chi}^\perp(q, q) \sim \frac{m^2}{Zq_0^2 + J_{\alpha\beta} q_\alpha q_\beta + hm} \quad (45)$$

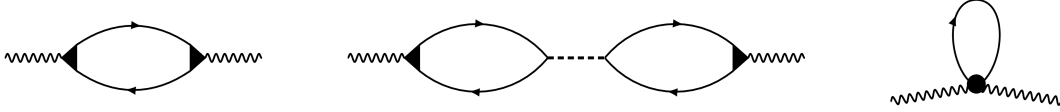


Figure 1. Feynman diagrams representing the RPA contributions to the gauge kernel: bare paramagnetic contribution, interaction correction, diamagnetic contribution.

for small  $q$ .

In Appendix A we derive another Ward identity for a *modified* gauge kernel  $\bar{K}_{\mu\nu}^{ab}$ , which is related to  $K_{\mu\nu}^{ab}$  by a Legendre transform.

### E. Spinon stiffnesses

We now derive expressions for the spin stiffnesses from the general formulae (13) and (14) in the case where the chargons are stripe ordered. The gauge kernel  $K_{\mu\nu}^{ab}$  is determined by two-point and four-point expectation values of chargon operators via Eq. (12). We compute the diamagnetic contribution in mean-field theory, and the paramagnetic contribution in random phase approximation (RPA), which is the conserving approximation for four point functions consistent with mean-field theory for the free energy and the Green function [54]. The RPA consists of a plain mean-field contribution and an interaction correction. The former can be represented diagrammatically by a bubble diagram, the latter by a pair of bubble diagrams connected by an effective interaction, see Fig. 1.

#### 1. Bare contributions

The “bare” paramagnetic gauge kernel, associated with the bubble diagram, has the form

$$K_{0,\mu\nu}^{p,ab}(q) = \frac{1}{4} \int_{k,k'} \text{tr} [\gamma_{\mathbf{k}+\mathbf{q}}^{\mu,a} G(k+q, k'+q) \gamma_{\mathbf{k}'}^{\nu,b} G(k', k)], \quad (46)$$

where  $\gamma_{\mathbf{k}}^{\mu,a} = \gamma_{\mathbf{k}}^{\mu} \sigma^a$ , and

$$G(k, k') = \begin{pmatrix} G_{\uparrow\uparrow}(k, k') & G_{\uparrow\downarrow}(k, k') \\ G_{\downarrow\uparrow}(k, k') & G_{\downarrow\downarrow}(k, k') \end{pmatrix}. \quad (47)$$

To evaluate Eq. (46) in a stripe state, we express the vertices and the Green functions in the spin-momentum basis  $\mathcal{B} = (\mathcal{B}_\uparrow, \mathcal{B}_\downarrow)$  with

$$\begin{aligned}\mathcal{B}_\uparrow &= (\mathbf{k}\uparrow, \mathbf{k} + \mathbf{Q}_1\downarrow, \mathbf{k} + \mathbf{Q}_2\uparrow, \dots, \mathbf{k} + \mathbf{Q}_{P-1}\downarrow), \\ \mathcal{B}_\downarrow &= (\mathbf{k}\downarrow, \mathbf{k} + \mathbf{Q}_1\uparrow, \mathbf{k} + \mathbf{Q}_2\downarrow, \dots, \mathbf{k} + \mathbf{Q}_{P-1}\uparrow),\end{aligned}\tag{48}$$

where the momentum  $\mathbf{k}$  is restricted to the reduced Brillouin zone of the stripe state. In this basis, the vertices are given by the  $2P \times 2P$  matrices

$$\Gamma_{\mathbf{k}}^{\mu,1} = \begin{pmatrix} 0 & \Gamma_{\mathbf{k}}^{\mu,+} \\ \Gamma_{\mathbf{k}}^{\mu,+} & 0 \end{pmatrix},\tag{49a}$$

$$\Gamma_{\mathbf{k}}^{\mu,2} = \begin{pmatrix} 0 & -i\Gamma_{\mathbf{k}}^{\mu,-} \\ i\Gamma_{\mathbf{k}}^{\mu,-} & 0 \end{pmatrix},\tag{49b}$$

$$\Gamma_{\mathbf{k}}^{\mu,3} = \begin{pmatrix} \Gamma_{\mathbf{k}}^{\mu,-} & 0 \\ 0 & -\Gamma_{\mathbf{k}}^{\mu,-} \end{pmatrix}.\tag{49c}$$

with the  $P \times P$  matrices

$$\Gamma_{\mathbf{k}}^{\mu,\pm} = \text{diag} \left( \gamma_{\mathbf{k}}^{\mu}, \pm\gamma_{\mathbf{k}+\mathbf{Q}_1}^{\mu}, \gamma_{\mathbf{k}+\mathbf{Q}_2}^{\mu}, \dots, \pm\gamma_{\mathbf{k}+\mathbf{Q}_{P-1}}^{\mu} \right).\tag{50}$$

The Green function also becomes a  $2P \times 2P$  matrix in the basis  $\mathcal{B}$ ,

$$\mathcal{G}(k) = \text{diag}[\mathcal{G}_\uparrow(k), \mathcal{G}_\downarrow(k)],\tag{51}$$

where  $\mathcal{G}_\uparrow(k)$  and  $\mathcal{G}_\downarrow(k)$  are the (identical)  $P \times P$  matrix Green functions defined in Eq. (29).

The bare paramagnetic gauge kernel in Eq. (46) can then be written as

$$K_{0,\mu\nu}^{p,ab}(q) = \frac{1}{4}T \sum_{k_0} \int_{\mathbf{k}} \text{tr} [\Gamma_{\mathbf{k}+\mathbf{q}}^{\mu,a} \mathcal{G}(k+q) \Gamma_{\mathbf{k}}^{\nu,b} \mathcal{G}(k)],\tag{52}$$

where the momentum integral extends over the reduced Brillouin zone. Inserting Eqs. (49) and (51) with the eigenvalue decomposition Eq. (30), and performing the Matsubara sum, one obtains

$$K_{0,\mu\nu}^{p,11}(q) = \frac{1}{2} \int_{\mathbf{k}} \sum_{\ell,\ell'} \text{tr} (\Gamma_{\mathbf{k}+\mathbf{q}}^{\mu,+} g_{\mathbf{k}+\mathbf{q}}^{\ell} \Gamma_{\mathbf{k}}^{\nu,+} g_{\mathbf{k}}^{\ell'}) \frac{f(E_{\mathbf{k}+\mathbf{q}}^{\ell}) - f(E_{\mathbf{k}}^{\ell'})}{iq_0 + E_{\mathbf{k}+\mathbf{q}}^{\ell} - E_{\mathbf{k}}^{\ell'}},\tag{53}$$

$$\begin{aligned}K_{0,\mu\nu}^{p,22}(q) &= K_{0,\mu\nu}^{p,33}(q) \\ &= \frac{1}{2} \int_{\mathbf{k}} \sum_{\ell,\ell'} \text{tr} (\Gamma_{\mathbf{k}+\mathbf{q}}^{\mu,-} g_{\mathbf{k}+\mathbf{q}}^{\ell} \Gamma_{\mathbf{k}}^{\nu,-} g_{\mathbf{k}}^{\ell'}) \frac{f(E_{\mathbf{k}+\mathbf{q}}^{\ell}) - f(E_{\mathbf{k}}^{\ell'})}{iq_0 + E_{\mathbf{k}+\mathbf{q}}^{\ell} - E_{\mathbf{k}}^{\ell'}},\end{aligned}\tag{54}$$

while all the off-diagonal components  $K_{0,\mu\nu}^{p,ab}(q)$  with  $a \neq b$  vanish.

The diamagnetic contribution to the gauge kernel is given by

$$K_{\alpha\beta}^{d,ab} = \frac{1}{4}\delta_{ab} \int_k \gamma_{\mathbf{k}}^{\alpha\beta} \text{tr}[G(k, k)], \quad (55)$$

where  $G$  is the chargin Green function computed in mean-field theory. It has only spatial components, that is,  $\alpha, \beta \in \{x, y\}$ . In the stripe order basis  $\mathcal{B}$ , the diamagnetic vertex has the  $2P \times 2P$  matrix structure

$$\Gamma_{\mathbf{k}}^{d,\alpha\beta} = \begin{pmatrix} \Gamma_{\mathbf{k}}^{\alpha\beta} & 0 \\ 0 & \Gamma_{\mathbf{k}}^{\alpha\beta} \end{pmatrix}, \quad (56)$$

with the  $P \times P$  matrix

$$\Gamma_{\mathbf{k}}^{\alpha\beta} = \text{diag} \left( \gamma_{\mathbf{k}}^{\alpha\beta}, \gamma_{\mathbf{k}+\mathbf{Q}_1}^{\alpha\beta}, \gamma_{\mathbf{k}+\mathbf{Q}_2}^{\alpha\beta}, \dots, \gamma_{\mathbf{k}+\mathbf{Q}_{P-1}}^{\alpha\beta} \right). \quad (57)$$

The diamagnetic gauge kernel can thus be written as

$$K_{\alpha\beta}^{d,ab} = \frac{1}{4}\delta_{ab} T \sum_{k_0} \int_{\mathbf{k}} \text{tr} \left[ \Gamma_{\mathbf{k}}^{\alpha\beta} \mathcal{G}(k) \right]. \quad (58)$$

Inserting Eq. (51) with the eigenvalue decomposition Eq. (30), and performing the Matsubara sum, one obtains

$$K_{\alpha\beta}^{d,ab} = \frac{1}{2}\delta_{ab} \int_{\mathbf{k}} \sum_{\ell} \text{tr} \left( \Gamma_{\mathbf{k}}^{\alpha\beta} g_{\mathbf{k}}^{\ell} \right) f(E_{\mathbf{k}}^{\ell}). \quad (59)$$

We now compute the spatial stiffnesses by taking the limits  $\mathbf{q} \rightarrow 0$  and  $q_0 \rightarrow 0$  as in Eq. (13). For the bare paramagnetic contribution the symmetry breaking external field  $h$  is irrelevant and can be set equal to zero from the beginning. The diamagnetic contribution is a momentum and frequency independent constant. The bare paramagnetic contribution to the spatial stiffnesses is obtained as

$$\begin{aligned} J_{0,\alpha\beta}^{p,11} &= \lim_{\mathbf{q} \rightarrow \mathbf{0}} K_{0,\alpha\beta}^{p,11}(\mathbf{q}, 0) \\ &= \frac{1}{2} \int_{\mathbf{k}} \sum_{\ell, \ell'} \text{tr}(\Gamma_{\mathbf{k}}^{\alpha,+} g_{\mathbf{k}}^{\ell} \Gamma_{\mathbf{k}}^{\beta,+} g_{\mathbf{k}}^{\ell'}) \left[ \delta_{\ell\ell'} f'(E_{\mathbf{k}}^{\ell}) + (1 - \delta_{\ell\ell'}) \frac{f(E_{\mathbf{k}}^{\ell}) - f(E_{\mathbf{k}}^{\ell'})}{E_{\mathbf{k}}^{\ell} - E_{\mathbf{k}}^{\ell'}} \right], \end{aligned} \quad (60)$$

$$\begin{aligned} J_{0,\alpha\beta}^{p,22} &= J_{0,\alpha\beta}^{p,33} = \lim_{\mathbf{q} \rightarrow \mathbf{0}} K_{0,\alpha\beta}^{p,22}(\mathbf{q}, 0) = \lim_{\mathbf{q} \rightarrow \mathbf{0}} K_{0,\alpha\beta}^{p,33}(\mathbf{q}, 0) \\ &= \frac{1}{2} \int_{\mathbf{k}} \sum_{\ell, \ell'} \text{tr}(\Gamma_{\mathbf{k}}^{\alpha,-} g_{\mathbf{k}}^{\ell} \Gamma_{\mathbf{k}}^{\beta,-} g_{\mathbf{k}}^{\ell'}) \left[ \delta_{\ell\ell'} f'(E_{\mathbf{k}}^{\ell}) + (1 - \delta_{\ell\ell'}) \frac{f(E_{\mathbf{k}}^{\ell}) - f(E_{\mathbf{k}}^{\ell'})}{E_{\mathbf{k}}^{\ell} - E_{\mathbf{k}}^{\ell'}} \right]. \end{aligned} \quad (61)$$

In Appendix B we show that  $J_{0,\alpha\beta}^{p,11} = -K_{\alpha\beta}^{d,11}$ , so that the diamagnetic and the bare paramagnetic contributions to  $J_{\alpha\beta}^{11}$  cancel each other.

The temporal stiffness  $Z^{ab}$  defined in Eq. (14) has only paramagnetic contributions. The bare contributions are obtained from Eqs. (53) and (54) as

$$Z_0^{11} = -\frac{1}{2} \int_{\mathbf{k}} \sum_{\ell \neq \ell'} \text{tr}(\Gamma^{0,+} g_{\mathbf{k}}^{\ell} \Gamma^{0,+} g_{\mathbf{k}}^{\ell'}) \frac{f(E_{\mathbf{k}}^{\ell}) - f(E_{\mathbf{k}}^{\ell'})}{E_{\mathbf{k}}^{\ell} - E_{\mathbf{k}}^{\ell'}} = 0, \quad (62)$$

$$Z_0^{22} = -\frac{1}{2} \int_{\mathbf{k}} \sum_{\ell \neq \ell'} \text{tr}(\Gamma^{0,-} g_{\mathbf{k}}^{\ell} \Gamma^{0,-} g_{\mathbf{k}}^{\ell'}) \frac{f(E_{\mathbf{k}}^{\ell}) - f(E_{\mathbf{k}}^{\ell'})}{E_{\mathbf{k}}^{\ell} - E_{\mathbf{k}}^{\ell'}} = Z_0^{33}. \quad (63)$$

The vertices  $\Gamma^{0,\pm}$  are momentum independent. The first component  $Z_0^{11}$  vanishes because  $\Gamma^{0,+}$  is the identity matrix and  $\text{tr}(g_{\mathbf{k}}^{\ell} g_{\mathbf{k}}^{\ell'}) = 0$  for  $\ell \neq \ell'$ .

## 2. Interaction correction

The interaction correction to  $K_{\mu\nu}^{ab}(q)$  has the form

$$\Delta K_{\mu\nu}^{ab}(q) = \int_{q',q''} \sum_{c,d} K_{0,\mu 0}^{p,ac}(q,q') \Gamma^{cd}(q',q'') K_{0,0\nu}^{p,db}(q'',q), \quad (64)$$

where  $K_{0,\mu\nu}^{p,ab}(q,q')$  is the bare paramagnetic gauge kernel with arbitrary ingoing and outgoing momenta, and  $\Gamma$  is the RPA effective interaction. The latter is determined by the linear integral equation

$$\Gamma^{cd}(q,q') = \Gamma_0^{cd} + \int_{q''} \sum_{c'd'} \Gamma_0^{cc'} \chi_0^{c'd'}(q,q'') \Gamma^{d'd}(q'',q'), \quad (65)$$

with the bare interaction  $\Gamma_0 = 2 \text{diag}(-\bar{U}, \bar{U}, \bar{U}, \bar{U})$ , and the bare susceptibility  $\chi_0^{cd}(q,q') = -K_{0,00}^{cd}(q,q') = -K_{0,00}^{p,cd}(q,q')$ . While the calculation of the stiffnesses requires only the spin SU(2) gauge kernel  $K_{\mu\nu}^{ab}(q)$  with indices  $a, b = 1, 2, 3$ , the effective interaction couples spin and charge, so that the indices  $c$  and  $d$  in Eqs. (64) and (65) are spin-charge indices, and the Pauli matrices in the spin channels are complemented by the unit matrix  $\sigma^0$  in the charge channel.

The above equations involve off-diagonal components of the bare gauge kernels, both in the momentum and spin variables. They are still given by bubble diagrams, but now the ingoing and outgoing momenta may differ by  $\mathbf{Q}_n = n(2\pi/p, \pi)$  with  $n = 0, \dots, P-1$ . Generalizing Eq. (46), we obtain

$$K_{0,\mu\nu}^{p,ab}(q,q') = \frac{1}{4} \int_{k,k'} \text{tr}[\gamma_{\mathbf{k}+\mathbf{q}}^{\mu,a} G(k+q, k'+q') \gamma_{\mathbf{k}'}^{\nu,b} G(k', k)], \quad (66)$$

where  $\gamma_{\mathbf{k}}^{\mu,a} = \gamma_{\mathbf{k}}^{\mu}\sigma^a$  now includes also the charge vertex for  $a = 0$ .

To solve the integral equation (65), and to evaluate  $\Delta K_{\mu\nu}^{ab}(q)$ , it is convenient to cast the off-diagonal momentum dependences in a matrix form. To this end, we substitute  $\mathbf{q} \rightarrow \mathbf{q} + \mathbf{Q}_n$ ,  $\mathbf{q}' \rightarrow \mathbf{q}' + \mathbf{Q}_{n'}$ , etc., and restrict the continuous part of the momenta to the magnetic Brillouin zone. Since  $K_{0,\mu\nu}^{p,ab}(q, q')$  and  $\Gamma^{cd}(q, q')$  are diagonal in the frequency variables  $q_0$  and  $q'_0$ , and also in the restricted momentum variables  $\mathbf{q}$  and  $\mathbf{q}'$ , we can substitute  $K_{0,\mu\nu}^{p,ab}(q, q') \rightarrow K_{0,\mu\nu}^{p,ab}(\mathbf{Q}_n, \mathbf{Q}_{n'}; q)$  and  $\Gamma^{cd}(q, q') \rightarrow \Gamma^{cd}(\mathbf{Q}_n, \mathbf{Q}_{n'}; q)$ . Eq. (64) can then be written as

$$\Delta K_{\mu\nu}^{ab}(q) = \sum_{c,d} \sum_{n',n''} K_{0,\mu 0}^{p,ac}(\mathbf{0}, \mathbf{Q}_{n'}; q) \Gamma^{cd}(\mathbf{Q}_{n'}, \mathbf{Q}_{n''}; q) K_{0,0\nu}^{p,db}(\mathbf{Q}_{n''}, \mathbf{0}; q), \quad (67)$$

and Eq. (65) becomes

$$\Gamma^{cd}(\mathbf{Q}_n, \mathbf{Q}_{n'}; q) = \Gamma_0^{cd} + \sum_{n''} \sum_{c'd'} \Gamma_0^{cc'} \chi_0^{c'd'}(\mathbf{Q}_n, \mathbf{Q}_{n''}; q) \Gamma^{d'd}(\mathbf{Q}_{n''}, \mathbf{Q}_{n'}; q). \quad (68)$$

Note that the external momentum  $\mathbf{q}$  in Eq. (64) can be assumed to lie in the magnetic Brillouin zone, since we are ultimately interested in the limit  $q \rightarrow 0$ . Defining  $4P \times 4P$  matrices  $\Gamma(q)$  and  $\chi_0(q)$  with matrix elements  $\Gamma_{nn'}^{cd}(q) = \Gamma^{cd}(\mathbf{Q}_n, \mathbf{Q}_{n'}; q)$  and  $\chi_0^{cd}(\mathbf{Q}_n, \mathbf{Q}_{n'}; q)$ , respectively, where  $n, c$  are row indices and  $n', d$  column indices, Eq. (68) can be formally solved as

$$\Gamma(q) = [1 - \Gamma_0 \chi_0(q)]^{-1} \Gamma_0, \quad (69)$$

with  $\Gamma_{0;nn'} = 2 \text{diag}(-\bar{U}, \bar{U}, \bar{U}, \bar{U}) \delta_{nn'}$ .

Using the matrix notation introduced in Sec. II E 1, the bare paramagnetic gauge kernel in Eq. (66) can be written as

$$K_{0,\mu\nu}^{p,ab}(\mathbf{Q}_n, \mathbf{Q}_{n'}; q) = \frac{1}{4} \int_k' \text{tr} \left[ \Gamma_{\mathbf{k}+\mathbf{q}+\mathbf{Q}_n}^{\mu,a} \Pi_n \mathcal{G}(k+q) \Pi_{n'}^t \Gamma_{\mathbf{k}}^{\nu,b} \mathcal{G}(k) \right], \quad (70)$$

where  $\Pi_n$  denotes a cyclic permutation by  $n$  in the bases  $\mathcal{B}_{\uparrow}$  and  $\mathcal{B}_{\downarrow}$ , so that  $\Pi_n \mathcal{G} \Pi_n^t$  denotes the matrix obtained from  $\mathcal{G} = \text{diag}(\mathcal{G}_{\uparrow}, \mathcal{G}_{\downarrow})$  by shifting the rows of each  $\mathcal{G}_{\sigma}$  by  $n$  and the columns by  $n'$ . This formula generalizes Eq. (52), which holds only in the special case  $\mathbf{Q}_n = \mathbf{Q}_{n'} = 0$ . In particular, the bare susceptibility  $\chi_0^{ab} = -K_{0,00}^{p,ab}$  can be written as

$$\chi_0^{ab}(\mathbf{Q}_n, \mathbf{Q}_{n'}; q) = -\frac{1}{4} \int_k' \text{tr} \left[ \Sigma^a \Pi_n \mathcal{G}(k+q) \Pi_{n'}^t \Sigma^b \mathcal{G}(k) \right], \quad (71)$$

where  $\Sigma^0$  is the  $2P \times 2P$  unit matrix, and  $\Sigma^a = \Gamma^{0,a}$  with  $a = 1, 2, 3$  are the Pauli matrices in the basis  $\mathcal{B}$ .

Using the eigenvalue decomposition (30) of  $\mathcal{G}_\sigma(k)$ , the Matsubara sum over  $k_0$  in Eq. (70) can be carried out. Continuing the Matsubara frequency  $q_0$  to real frequencies,  $iq_0 \rightarrow \omega + i0^+$ , we obtain

$$K_{0,\mu\nu}^{p,ab}(\mathbf{Q}_n, \mathbf{Q}_{n'}; \mathbf{q}, \omega) = \frac{1}{2} \int_{\mathbf{k}} \sum_{\ell, \ell'} A_{\mu\nu, \ell\ell'}^{ab}(\mathbf{Q}_n, \mathbf{Q}_{n'}; \mathbf{k}, \mathbf{q}) F_{\ell\ell'}(\mathbf{k}, \mathbf{q}, \omega), \quad (72)$$

with

$$A_{\mu\nu, \ell\ell'}^{ab}(\mathbf{Q}_n, \mathbf{Q}_{n'}; \mathbf{k}, \mathbf{q}) = \frac{1}{2} \text{tr} \left[ \Gamma_{\mathbf{k}+\mathbf{q}+\mathbf{Q}_n}^{\mu,a} \begin{pmatrix} \Pi_n g_{\mathbf{k}+\mathbf{q}}^\ell \Pi_{n'}^t & 0 \\ 0 & \Pi_n g_{\mathbf{k}+\mathbf{q}}^\ell \Pi_{n'}^t \end{pmatrix} \Gamma_{\mathbf{k}}^{\nu,b} \begin{pmatrix} g_{\mathbf{k}}^{\ell'} & 0 \\ 0 & g_{\mathbf{k}}^{\ell'} \end{pmatrix} \right], \quad (73)$$

and

$$F_{\ell\ell'}(\mathbf{k}, \mathbf{q}, \omega) = \frac{f(E_{\mathbf{k}}^\ell) - f(E_{\mathbf{k}+\mathbf{q}}^{\ell'})}{\omega + i0^+ + E_{\mathbf{k}}^\ell - E_{\mathbf{k}+\mathbf{q}}^{\ell'}}. \quad (74)$$

To compute the interaction correction to the stiffnesses, we need to take the limits  $\mathbf{q} \rightarrow \mathbf{0}$ ,  $q_0 \rightarrow 0$ , and  $h \rightarrow 0$  in the appropriate order, see Eqs. (13) and (14). We recall that  $h$  is a symmetry breaking field. Although the effective interaction diverges for  $\mathbf{q}, q_0, h \rightarrow 0$  due to its Goldstone poles, the correction to the gauge kernel remains generally finite, thanks to compensating zeros in the bare gauge kernels, between which  $\Gamma$  is sandwiched in Eq. (64). However, the limit value depends on the order in which  $\mathbf{q}$ ,  $q_0$ , and  $h$  are sent to zero. In the case of spiral order (including Néel order as a special case), it is possible to take the limits analytically, and derive manifestly finite interaction corrections to the stiffnesses [16, 40, 52]. The terms which are removed by the symmetry breaking field  $h$  have qualitatively the asymptotic form  $\frac{q^2}{q^2+h}$ , where  $q$  stands for the small momentum or frequency variable. They vanish if  $q \rightarrow 0$  before  $h \rightarrow 0$ , while giving a finite result in the opposite order of limits. For the case of stripe order with a period  $p > 2$  it seems difficult to isolate the singular terms by hand, and to derive analytic expressions for the stiffnesses. However, we can still isolate the singular terms numerically, by diagonalizing the matrix denominator  $1 - \Gamma_0 \chi_0(q)$  in Eq. (69). Some of the eigenvalues vanish for  $\mathbf{q}, q_0, h \rightarrow 0$ . We then project out the corresponding eigenspaces, and perform the matrix inversion only in the remaining orthogonal space, yielding the so-called pseudoinverse [55], which remains finite by construction. Inserting the resulting effective interaction into Eq. (67) simulates the limit defined with an external field  $h$ , without the need to actually calculate any quantity in the presence of  $h$ . The order of the limits  $\mathbf{q} \rightarrow \mathbf{0}$  and  $q_0 \rightarrow 0$  still matters, and must be performed as described in the defining equations (13) and (14) for the spatial and temporal stiffnesses, respectively.

Like the bare contributions, the interaction corrections to the stiffnesses  $\Delta J_{\mu\nu}^{11}$  and  $\Delta J_{\mu\nu}^{ab}$  with  $a \neq b$  vanish, while  $\Delta J_{\mu\nu}^{22} = \Delta J_{\mu\nu}^{33}$ . Hence, the total stiffness  $J_{\mu\nu}^{ab} = J_{0,\mu\nu}^{p,ab} + J_{0,\mu\nu}^{d,ab} + \Delta J_{\mu\nu}^{ab}$  has the diagonal matrix form

$$\mathcal{J}_{\mu\nu} = \text{diag}(0, J_{\mu\nu}, J_{\mu\nu}). \quad (75)$$

This simple form could have been obtained also directly from the symmetry breaking pattern  $\text{SU}(2) \rightarrow \text{U}(1)$ , where the residual  $\text{U}(1)$  symmetry of the broken  $\text{SU}(2)$  contains rotations around the axis of the collinear spin alignment (the  $x$ -axis in spin space in our convention). For a stripe state with Néel order along one of the  $x$  or  $y$  (spatial) directions, the off-diagonal spatial stiffness components vanish, that is,  $J_{xy} = J_{yx} = 0$ . The diagonal components  $J_{xx}$  and  $J_{yy}$  are not equal, except in the special case of the Néel state. We neglect the mixed spatio-temporal components  $J_{\alpha 0}$  and  $J_{0\beta}$ , which may occur due to Landau damping of the spin waves.

## F. Solution of nonlinear sigma model

We solve the nonlinear sigma model (16) in a saddle-point approximation in the  $\text{CP}^1$  representation, which becomes exact in a large  $N$  limit [41].

### 1. $\text{CP}^1$ representation

The matrix  $\mathcal{R}$  can be expressed as a triad of orthonormal unit vectors  $\mathcal{R} = (\hat{\mathbf{n}}^1, \hat{\mathbf{n}}^2, \hat{\mathbf{n}}^3)$ , which can be represented in terms of two complex Schwinger bosons  $z_\uparrow$  and  $z_\downarrow$  [56],

$$\hat{\mathbf{n}}^1 = z^* \vec{\sigma} z, \quad (76a)$$

$$\hat{\mathbf{n}}^- = z(i\sigma^2 \vec{\sigma}) z, \quad (76b)$$

$$\hat{\mathbf{n}}^+ = z^*(i\sigma^2 \vec{\sigma})^\dagger z^*, \quad (76c)$$

with  $z = (z_\uparrow, z_\downarrow)$  and  $\hat{\mathbf{n}}^\pm = \hat{\mathbf{n}}^2 \mp i\hat{\mathbf{n}}^3$ . The Schwinger bosons obey the constraint

$$z_\uparrow^* z_\uparrow + z_\downarrow^* z_\downarrow = 1. \quad (77)$$

The parametrization (76) is equivalent to

$$R = \begin{pmatrix} z_\uparrow & -z_\downarrow^* \\ z_\downarrow & z_\uparrow^* \end{pmatrix}. \quad (78)$$

Inserting this representation of  $\mathcal{R}$  into Eq. (16) with a stiffness matrix of the form  $\mathcal{J}_{\mu\nu} = \text{diag}(0, J_{\mu\nu}, J_{\mu\nu})$ , we obtain the CP<sup>1</sup> action

$$\mathcal{S}_{\text{CP}^1}[z, z^*] = \int dx \left[ 2J_{\mu\nu}[\partial_\mu z^*(x)]\partial_\nu z(x) - 2J_{\mu\nu}j_\mu(x)j_\nu(x) \right], \quad (79)$$

with the current density

$$j_\mu(x) = \frac{i}{2} [z^*(x)\partial_\mu z(x) - z(x)\partial_\mu z^*(x)]. \quad (80)$$

## 2. Large N limit and saddle point

The current-current interaction in Eq. (79) can be decoupled by a Hubbard-Stratonovich transformation with a U(1) gauge field  $\mathcal{A}_\mu$ , and the constraint (77) can be implemented by a Lagrange multiplier field  $\lambda$ , leading to the action [41]

$$\mathcal{S}_{\text{CP}^1}[z, z^*, \mathcal{A}_\mu, \lambda] = \int dx [2J_{\mu\nu}(D_\mu z)^*(D_\nu z) + i\lambda(z^*z - 1)], \quad (81)$$

where  $D_\mu = \partial_\mu - i\mathcal{A}_\mu$  is the covariant derivative. We have suppressed the space-time dependence of the fields to shorten the expression.

To perform a large  $N$  expansion, we extend the two-component field  $z = (z_\uparrow, z_\downarrow)$  to an  $N$ -component field  $z = (z_1, \dots, z_N)$ , and rescale it by a factor  $\sqrt{N/2}$  so that it now satisfies the local constraint

$$z^*(x)z(x) = \sum_{\sigma=1}^N z_\sigma^*(x)z_\sigma(x) = \frac{N}{2}. \quad (82)$$

To obtain a nontrivial limit  $N \rightarrow \infty$ , we rescale also the stiffnesses  $J_{\mu\nu}$  by a factor  $2/N$ , yielding the CP <sup>$N-1$</sup>  action

$$\mathcal{S}_{\text{CP}^{N-1}}[z, z^*, \mathcal{A}_\mu, \lambda] = \int dx [2J_{\mu\nu}(D_\mu z)^*(D_\nu z) + i\lambda(z^*z - N/2)]. \quad (83)$$

In the large  $N$  limit, the partition function of the CP <sup>$N-1$</sup>  model is dominated by a saddle point for the fields  $\mathcal{A}$  and  $\lambda$ , at which  $\mathcal{A}_\mu(x) = 0$ , and  $\lambda(x) = \lambda$  is uniform in space and time [41]. One can then read off the spinon propagator directly from the action (83),

$$D(q) = \langle z_\sigma^*(q)z_\sigma(q) \rangle = \frac{1}{2Z(m_s^2 + q_0^2) + 2J_{\alpha\beta}q_\alpha q_\beta}, \quad (84)$$

where  $2m_s^2 = i\lambda/Z$ . The Lagrange multiplier  $\lambda$  and thus the spinon mass  $m_s$  are fixed by taking the average of the constraint, leading to  $\langle z^*(x)z(x) \rangle = N/2$ . At finite temperatures,

and also for a quantum disordered ground state, there is no Bose condensate, that is  $\langle z(x) \rangle = 0$ , and the constraint leads to the condition

$$2 \int_q D(q) = \int_q \frac{1}{Z(m_s^2 + q_0^2) + J_{\alpha\beta} q_\alpha q_\beta} = 1, \quad (85)$$

which determines the spinon mass  $m_s$  as a function of  $Z$ ,  $J_{\alpha\beta}$ , and an ultraviolet cutoff. Choosing an isotropic momentum cutoff  $\Lambda_{\text{uv}}$ , and performing the Matsubara sum over  $q_0$ , the condition (85) can be written more explicitly as

$$\frac{1}{4\pi J} \int_0^{c_s \Lambda_{\text{uv}}} \frac{\epsilon d\epsilon}{\sqrt{m_s^2 + \epsilon^2}} \coth \left[ \sqrt{m_s^2 + \epsilon^2} / (2T) \right] = 1, \quad (86)$$

where

$$J = \sqrt{\det \begin{pmatrix} J_{xx} & J_{xy} \\ J_{yx} & J_{yy} \end{pmatrix}}, \quad (87)$$

is an ‘‘average’’ spin stiffness, and  $c_s = \sqrt{J/Z}$  the corresponding average spin wave velocity. For stripe order with a Néel pattern along one of the axes (in  $x$  or  $y$  direction), the off-diagonal components of  $J_{\alpha\beta}$  vanish, so that  $J = \sqrt{J_{xx} J_{yy}}$ .

The spinon propagator Eq. (84) can be written in the alternative form

$$D(q) = -\frac{1}{2Z} \frac{1}{(iq_0 - \omega_{\mathbf{q}})(iq_0 + \omega_{\mathbf{q}})}, \quad (88)$$

with the spinon dispersion

$$\omega_{\mathbf{q}} = \sqrt{m_s^2 + (J_{\alpha\beta} \mathbf{q}_\alpha \mathbf{q}_\beta) / Z}. \quad (89)$$

From this expression it is evident that  $D(q)$  describes propagating bosonic excitations with a gapped dispersion  $\omega_{\mathbf{q}}$ . For  $m_s \rightarrow 0$  one recovers the usual spin waves of an ordered magnet.

## G. Electron Green function

We now derive an expression for the electron Green function  $G^e$ , from which the spectral function for single-particle excitations can be obtained. The superscript ‘‘e’’ distinguishes the electron Green function from the chargin Green function  $G$ . The imaginary time electron Green function is defined as

$$G_{j\sigma, j'\sigma'}^e(\tau) = -\langle c_{j\sigma}(\tau) c_{j'\sigma'}^*(0) \rangle. \quad (90)$$

Inserting the fractionalization (2) of the electron fields, we obtain

$$G_{j\sigma,j'\sigma'}^e(\tau) = - \sum_{s,s'} \langle [R_j(\tau)]_{\sigma s} [R_{j'}^*(0)]_{\sigma's'} \psi_{js}(\tau) \psi_{j's'}^*(0) \rangle. \quad (91)$$

We simplify this expression by neglecting chargon-spinon interactions, so that we can decouple the expectation value as

$$G_{j\sigma,j'\sigma'}^e(\tau) = - \sum_{s,s'} \langle [R_j(\tau)]_{\sigma s} [R_{j'}^*(0)]_{\sigma's'} \rangle \langle \psi_{js}(\tau) \psi_{j's'}^*(0) \rangle. \quad (92)$$

This approximation is common in gauge theories of fluctuating magnetic order [13, 14, 16, 20]. The first expectation value is the spinon propagator, and the second one the chargon Green function in real space representation,  $G_{js,j's'}(\tau) = - \langle \psi_{js}(\tau) \psi_{j's'}^*(0) \rangle$ .

Using the Schwinger boson representation (78) of  $R$ , we obtain

$$\langle [R_j(\tau)]_{\sigma s} [R_{j'}^*(0)]_{\sigma's'} \rangle = \langle z_{j\sigma}(\tau) z_{j'\sigma'}^*(0) \rangle \delta_{\sigma\sigma'} \delta_{ss'} = D_{jj'}(\tau) \delta_{\sigma\sigma'} \delta_{ss'}, \quad (93)$$

in the saddle point approximation to the nonlinear sigma model, where  $D_{jj'}(\tau)$  is the Fourier transform of the spinon propagator  $D(q)$  in Eq. (84). The Kronecker deltas arise since expectation values of the form  $\langle z_\sigma z_{\sigma'} \rangle$  and  $\langle z_\uparrow^* z_\downarrow \rangle$  vanish due to the SU(2) symmetry of the nonlinear sigma model. Fourier transforming Eq. (92), we then obtain the electron Green function in momentum representation,  $G_{\sigma\sigma'}^e(\mathbf{k}, \mathbf{k}', ik_0) = G^e(\mathbf{k}, \mathbf{k}', ik_0) \delta_{\sigma\sigma'}$ , where

$$G^e(\mathbf{k}, \mathbf{k}', ik_0) = T \sum_{q_0} \int_{\mathbf{q}} \sum_s G_{ss}(\mathbf{k} - \mathbf{q}, \mathbf{k}' - \mathbf{q}, ik_0 - iq_0) D(\mathbf{q}, iq_0). \quad (94)$$

At this point we see that the electron Green function is SU(2) symmetric, that is, the spinon fluctuations restore the broken SU(2) symmetry of the chargons. However, the translation symmetry remains partially broken, that is,  $G^e(\mathbf{k}, \mathbf{k}', ik_0)$  has momentum off-diagonal contributions for  $\mathbf{k}' - \mathbf{k} = \mathbf{Q}_n$  with even  $n$ . This is due to the charge order of the stripes, which is not removed by the spinon fluctuations. By contrast, in a fluctuating spiral magnet there is no charge order, and the electron Green function recovers the full translation invariance of the lattice [16]. Substituting  $\mathbf{k} \rightarrow \mathbf{k} + \mathbf{Q}_n$  and  $\mathbf{k}' \rightarrow \mathbf{k}' + \mathbf{Q}_{n'}$ , where  $\mathbf{k}$  and  $\mathbf{k}'$  are situated in the first magnetic Brillouin zone, we have  $\mathbf{k} = \mathbf{k}'$  and the momentum dependence of the electron Green function can be parametrized as  $G^e(\mathbf{Q}_n, \mathbf{Q}_{n'}; \mathbf{k}, ik_0)$ , with  $n' - n$  even.

Using the eigenvalue decomposition Eq. (30) of the chargon Green function, the Matsubara sum in Eq. (94) can be carried out, and the analytic continuation  $ik_0 \rightarrow \omega + i0^+$  can

be performed explicitly. After some straightforward algebra we obtain the electron Green function in its final form,

$$G^e(\mathbf{Q}_n, \mathbf{Q}_{n'}; \mathbf{k}, \omega) = \int_{\mathbf{q}} \sum_{\ell} \sum_{p=\pm} \frac{1}{2Z\omega_{\mathbf{q}}} \frac{b(\omega_{\mathbf{q}}) + f(pE_{\mathbf{k}-\mathbf{q}}^{\ell})}{\omega + i0^+ - E_{\mathbf{k}-\mathbf{q}}^{\ell} + p\omega_{\mathbf{q}}} (g_{\mathbf{k}-\mathbf{q}}^{\ell})_{nn'}. \quad (95)$$

The momentum integral over  $\mathbf{q}$  is restricted by the same ultraviolet cutoff as the momentum integral of the constraint Eq. (85).

In the special case of Néel order, that is, for  $P = 2$ , the electron Green function is translation invariant, and the contributing spectral weights have the form  $(g_{\mathbf{k}}^{\ell})_{00} = 1 + \ell h_{\mathbf{k}}/e_{\mathbf{k}}$  and  $(g_{\mathbf{k}}^{\ell})_{11} = 1 + \ell h_{\mathbf{k}+\mathbf{Q}}/e_{\mathbf{k}+\mathbf{Q}}$ , where  $h_{\mathbf{k}} = \frac{1}{2}(\epsilon_{\mathbf{k}} - \epsilon_{\mathbf{k}+\mathbf{Q}})$  and  $e_{\mathbf{k}} = \sqrt{\Delta^2 + h_{\mathbf{k}}^2}$ . The expression (95) then agrees with the corresponding expression for a spiral magnet in the Néel limit  $\mathbf{Q} \rightarrow (\pi, \pi)$  derived in Ref. [16].

### III. RESULTS

We now present and discuss results obtained from the SU(2) gauge theory of fluctuating stripe order for some specific choices of model parameters. Defining the nearest neighbor hopping  $t$  as our energy unit, we consider three choices for the next-to-nearest neighbor hopping:  $t' = 0$ ,  $t' = -0.15t$  and  $t' = -0.3t$ . The first one, corresponding to pure nearest neighbor hopping, is not adequate for cuprate superconductors, but has nevertheless been a popular choice for numerical simulations of the Hubbard model, favoring especially stripe order [31–34]. A next-nearest neighbor hopping  $t' = -0.15t$  is frequently used to model the band structure of the LSCO family of cuprate superconductors, and  $t' = -0.3t$  for YBCO [57]. For the Hubbard interaction we choose a moderate value  $U = 5t$ . Applying the functional RG flow as described in Sec. II C, the corresponding effective interactions  $\bar{U}(n)$  are about one half of the bare values, see Fig. 2. We choose the nearest neighbor hopping amplitude  $t$  as our energy unit, setting  $t = 1$  in the figures.

Our main result is the spectral function for single-particle excitations, as obtained from the imaginary part of the electron Green function. To understand this result, we first discuss its ingredients, namely the stripe order of the chargons and the corresponding pseudospin stiffnesses.

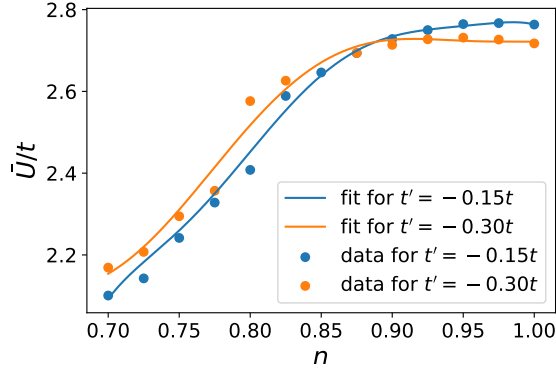


Figure 2. Effective interaction  $\bar{U}$  as a function of density for  $t' = -0.15t$  and  $t' = -0.3t$ . The polynomial fit is used for  $\bar{U}(n)$  in all subsequent results. The bare interaction is  $U = 5t$  in all plots.

### A. Stripe ordered chargons

The chargons are treated in renormalized mean-field theory, see Sec. II C. We ignore superconductivity and focus on regions in the phase diagram where unidirectional stripe order minimizes the free energy. Pseudogap behavior in regions with Néel or spiral order has already been analyzed previously within our SU(2) gauge theory of fluctuating magnetic order [16, 17]. For sizable values of  $t'/t$ , the magnetic order is of stripe-type only for a sizable hole doping below half-filling ( $n < 1$ ). For electron doping ( $n > 1$ ) and small hole doping, the magnetic order is of Néel-type or spiral, respectively [29, 30].

As explained in Sec. II C 2, we need to assume a *commensurate* stripe order with a finite period  $p$  in our numerical calculations. The order is then characterized by real space spin and charge profiles, which are described by finite Fourier series with wave vectors  $\mathbf{Q}_n = (2\pi n/p, n\pi)$  with  $n \in \{0, 1, \dots, P-1\}$ , where  $P = p$  if  $p$  is even, and  $P = 2p$  if  $p$  is odd. The spin profile is described by Fourier coefficients  $M_n$  with odd  $n$ , and the charge profile by coefficients  $\rho_n$  with even  $n$ . The gap equations determine the Fourier coefficients  $M_n$  and  $\rho_n$  for any given period  $p$ , and we select the optimal period  $p$  by minimizing the free energy with respect to  $p$ , offering the following choices:  $p \in \{2, 3, \dots, 16\}$ . Momentum integrals are replaced by discrete momentum sums corresponding to very large lattices (several hundred sites in each direction) with periodic boundary conditions and linear dimensions in  $x$  direction which are integer multiples of  $p$ .

The spin and charge profiles are never strictly harmonic, but rather a superposition with

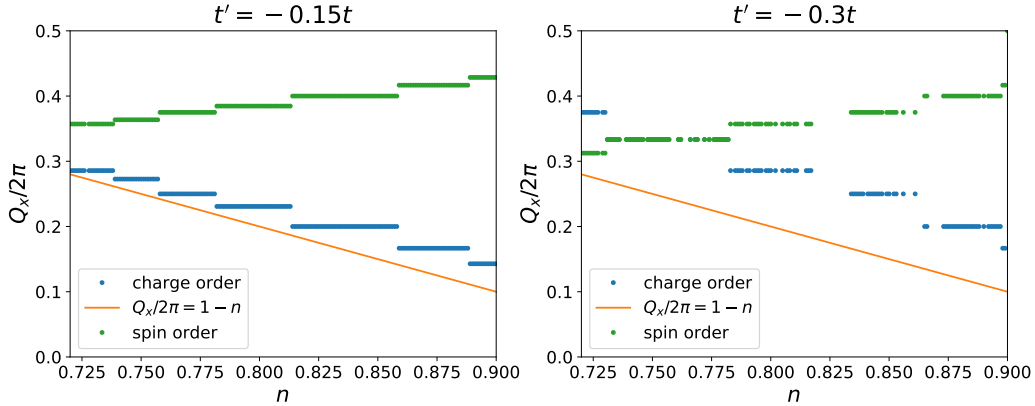


Figure 3.  $x$  coordinates of the dominant charge and spin ordering wave vectors as a function of the electron density  $n$  for  $U = 5t$  and  $T = 0.02t$ . Left:  $t' = -0.15$ , right:  $t' = -0.3t$ .

several wave vectors  $\mathbf{Q}_n$ . We refer to the wave vectors with the largest Fourier coefficients  $|M_n|$  and  $|\rho_n|$  as the *dominant* spin and charge order wave vectors  $\mathbf{Q}^s$  and  $\mathbf{Q}^c$ , respectively. Strictly speaking there are inversion-symmetry related pairs of dominant wave vectors with equally maximal  $|M_n|$  and  $|\rho_n|$  for spin and charge, respectively. The  $y$  component of  $\mathbf{Q}^s$  and  $\mathbf{Q}^c$  is always  $\pi$  and  $0$ , respectively. The choice of  $\mathbf{Q}^s$  and  $\mathbf{Q}^c$  becomes unique if we consider only wave vectors with an  $x$  component between  $0$  and  $\pi$ . In Fig. 3 we show the  $x$  components of the dominant ordering wave vectors  $\mathbf{Q}^s$  and  $\mathbf{Q}^c$  with  $0 \leq Q_x^{s,c} < \pi$  as a function of the electron density at a fixed temperature  $T = 0.02t$  for two choices of  $t'$ . The dominant charge order wave vector exhibits an almost linear density dependence over a broad density range. Its form of a discontinuous step function is an artifact of the limited number of periodicities  $p$  we can offer. For  $t' = 0$  (not shown in the figure), the dominant charge order wave vector closely follows the line  $Q_x = 2\pi(1 - n)$ , while for  $t' = -0.15$  and  $t' = -0.3t$  there is a constant offset. The  $x$  component of  $\mathbf{Q}^s$  also varies roughly linearly with density, except near the edges of the stripe regime. For  $t' = 0$ , where stripe order is stable up to half-filling,  $Q_x^s$  converges to  $\pi$  for  $n \rightarrow 1$ , approaching thus smoothly the half-filled Néel state.

In Fig. 4 we show the quasi-particle Fermi surfaces defined as zeros of the quasi-particle bands  $E_{\mathbf{k}}^\ell$  in the full Brillouin zone (repeated zone scheme) for two distinct stripe periodicities  $p$ . The Fermi surface of the corresponding non-interacting system is shown in the same repeated zone scheme for comparison. It consists of the original bare Fermi surface and its

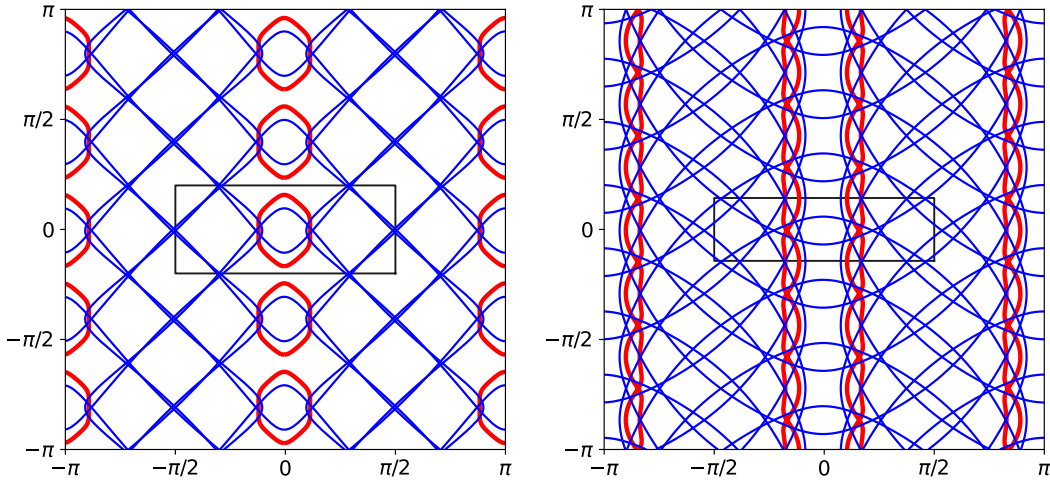


Figure 4. Quasi-particle Fermi surfaces (red lines) of two stripe states with periodicities  $p = 5$  (left) and  $p = 14$  (right), presented in the full Brillouin zone (repeated zone scheme). The Fermi surface of the corresponding non-interacting system (blue lines) is shown in the same repeated zone scheme for comparison. The black box in the center indicates the (reduced) magnetic Brillouin zones corresponding to the reduced translation invariance of the stripe ordered state. Parameters:  $t' = -0.15t$ ,  $n = 0.83$ ,  $T = 0.02t$  (left),  $t' = -0.3t$ ,  $n = 0.799$ ,  $T = 0.02t$  (right).

copies obtained from a shift by  $\mathbf{Q}_n$  with  $n = 1, \dots, P - 1$ . Some of the quasi-particle bands  $E_{\mathbf{k}}^{\ell}$  are completely filled, and others are completely empty. Hence, generally only some of the bands are *partially* filled and form a Fermi surface sheet. A large magnetic gap favors a reduced number of partially filled bands (while most bands are either completely filled or empty). In the left panel of Fig. 4, only one of the ten quasi-particle bands is partially filled, leading to a relatively simple Fermi surface topology with a single electron pocket in the reduced Brillouin zone. In the right panel, two of the fourteen quasi-particle bands are partially filled, and the Fermi surface consists of various open lines, as if the system was quasi one-dimensional. For a slightly higher filling (not shown), pockets appear in addition to the open lines. Quite generally, the shape of the Fermi surfaces can change significantly upon small changes of the density.

## B. Stiffnesses

In Figs. 5 and 6 we show the spatial stiffness in  $x$  direction  $J_{xx}$  and the temporal stiffness  $Z$  as functions of density in the stripe ordered regime for various low temperatures,  $U = 5t$ , and two choices of  $t'$ . The spatial stiffness in  $y$  direction behaves similarly. The indicated periodicities  $p$  minimize the free energy within the set  $p \in \{1, 2, \dots, 16\}$ . We show the stiffnesses only in the density interval in which stripe order is the energetically most favorable magnetic order. The spatial stiffness varies quite rapidly as a function of density, and very low values are obtained at certain densities even at the lowest temperatures. For  $t' = -0.3t$ , there are densities for which none of the available periodicities lead to a state with a positive spatial stiffness. This is due to the limited set of periodicities we can offer, which limits the set of allowed wave vectors  $\mathbf{Q}_n$ . Discarding the irregularities resulting from this restriction, one can see that the highest data points (for each temperature) in the figures follow regular envelopes, which define the stiffnesses one should obtain in the thermodynamic limit, if arbitrary periodicities were allowed.

The size of the stiffnesses (deep inside the stripe regime) is of the same order of magnitude as the ones in the Néel state at half-filling [58, 59]. The stiffnesses consist of a “bare” contribution and an interaction correction (see Secs. II E 1 and II E 2). The latter, which is much harder to compute, is generally much smaller than the former.

## C. Electron spectral function

We now present results for the spectral function for single-particle excitations, which is directly related to the imaginary part of the electron Green function by

$$A(\mathbf{k}, \mathbf{k}', \omega) = -\frac{1}{\pi} \text{Im} G^e(\mathbf{k}, \mathbf{k}', \omega + i0^+). \quad (96)$$

We focus on its momentum diagonal part, which, via Eq. (95), can be written as

$$\begin{aligned} A(\mathbf{k}, \omega) &= -\frac{1}{\pi} \text{Im} G^e(\mathbf{0}, \mathbf{0}; \mathbf{k}, \omega) \\ &= \int_{\mathbf{q}} \sum_{\ell} \sum_{p=\pm} \frac{1}{2Z\omega_{\mathbf{q}}} [b(\omega_{\mathbf{q}}) + f(pE_{\mathbf{k}-\mathbf{q}}^{\ell})] (g_{\mathbf{k}-\mathbf{q}}^{\ell})_{00} \delta(\omega + i0^+ - E_{\mathbf{k}-\mathbf{q}}^{\ell} + p\omega_{\mathbf{q}}). \end{aligned} \quad (97)$$

$A(\mathbf{k}, \omega)$  can be measured by angular resolved photoemission [60].

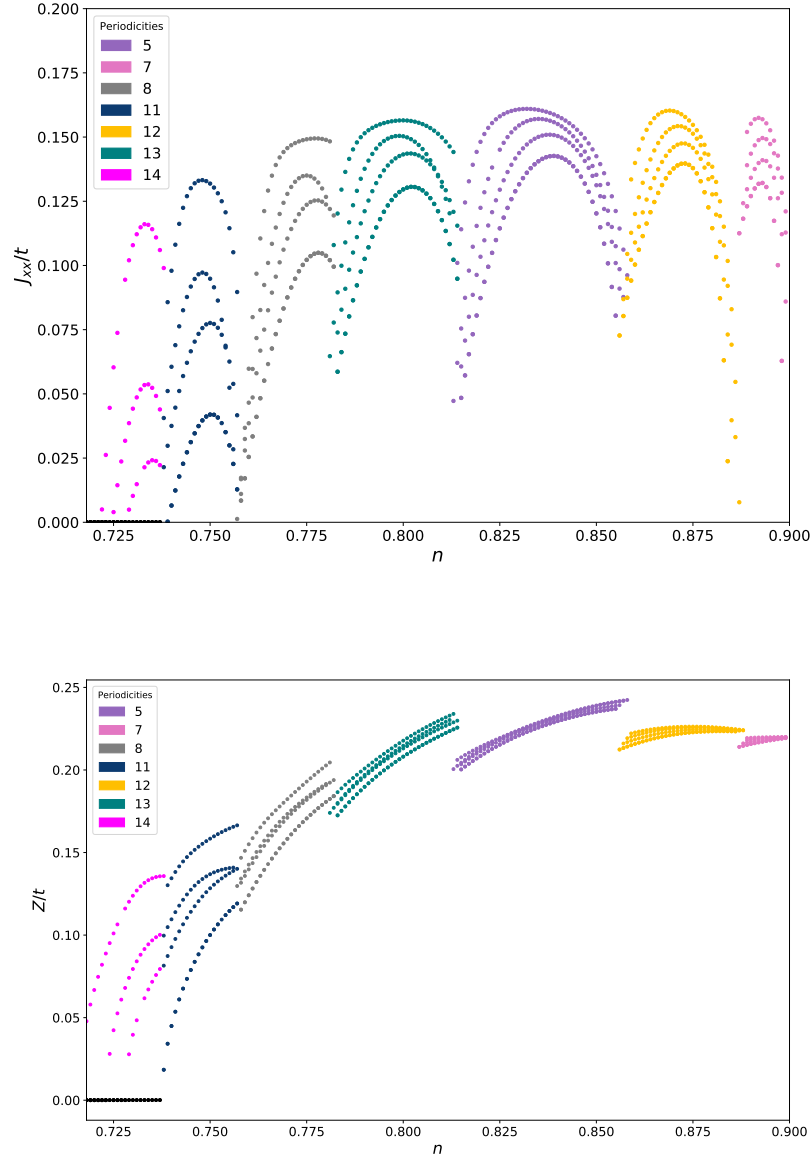


Figure 5. Spatial stiffness in  $x$  direction  $J_{xx}$  and temporal stiffness  $Z$  as functions of density in the stripe ordered regime for  $t' = -0.15t$  and various low temperatures  $T = 0.02t, 0.03t, 0.04t, 0.05t$ . The periodicities  $p$  of the stripe order, which minimize the free energy within the restricted set  $p \in \{1, 2, \dots, 16\}$ , are indicated by different colors. Larger stiffnesses (at a given density) correspond to lower temperatures.

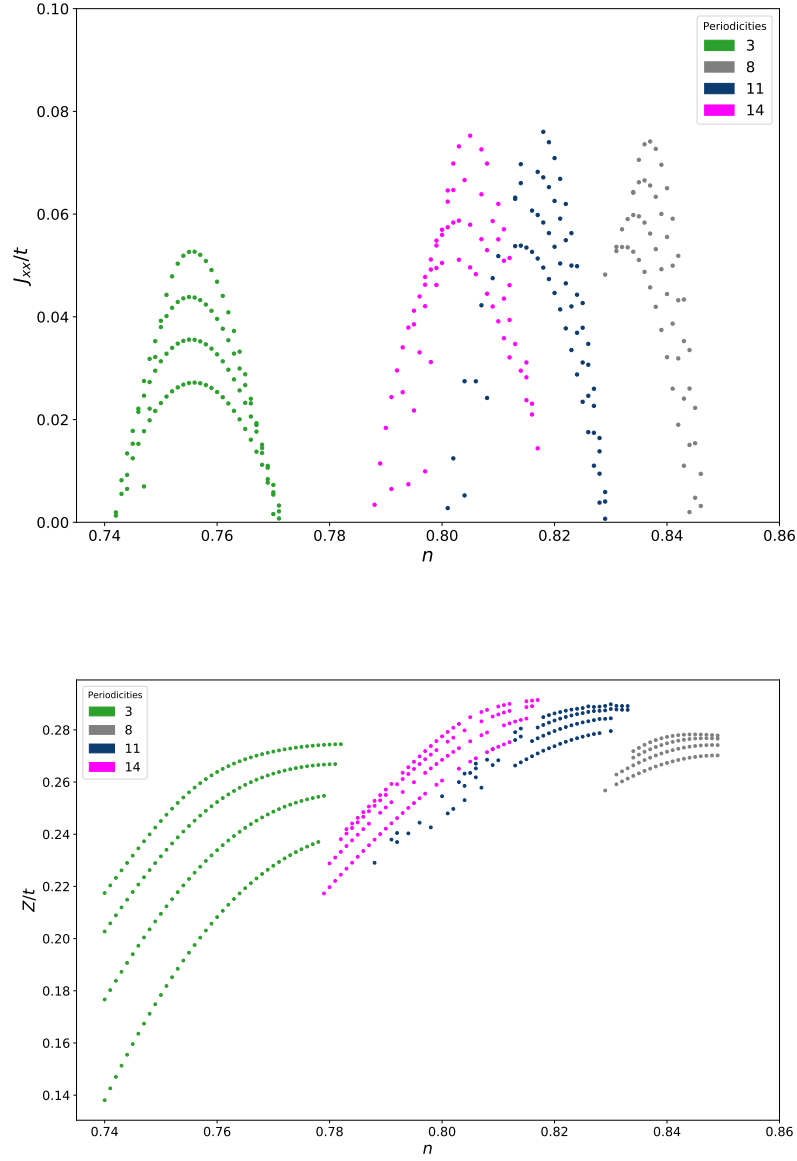


Figure 6. Spatial stiffness in  $x$  direction  $J_{xx}$  and temporal stiffness  $Z$  as functions of density in the stripe ordered regime for  $t' = -0.3t$  and various low temperatures  $T = 0.02t, 0.03t, 0.04t, 0.05t$ . The periodicities  $p$  of the stripe order, which minimize the free energy within the restricted set  $p \in \{1, 2, \dots, 16\}$ , are indicated by different colors. Larger stiffnesses (at a given density) correspond to lower temperatures.

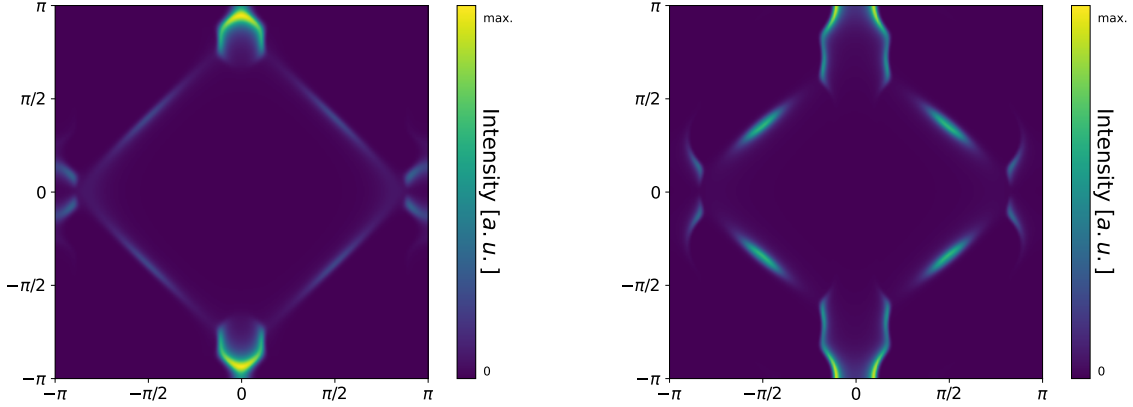


Figure 7. Spectral function for single-particle excitations  $A(\mathbf{k}, \omega)$  at  $\omega = 0$ . Parameters:  $t' = -0.15t$ ,  $n = 0.83$ ,  $T = 0.02t$  (left),  $t' = -0.3t$ ,  $n = 0.799$ ,  $T = 0.02t$  (right).

In Fig. 7 we show the spectral function  $A(\mathbf{k}, \omega)$  at  $\omega = 0$  for two distinct cases of fluctuating stripe order. The parameters are the same as in Fig. 4. In a normal Fermi liquid,  $A(\mathbf{k}, 0)$  exhibits a pronounced peak at the Fermi surface. In a state with magnetic and/or charge order,  $A(\mathbf{k}, 0)$  is peaked at the (reconstructed) Fermi surface of the quasi-particles. The size of the peaks is strongly momentum dependent, due to weight factors which are very small for momenta  $\mathbf{k}$  remote from the bare Fermi surface [22]. The spinon fluctuations broaden the peaks to some extent. Indeed, the spectral functions  $A(\mathbf{k}, 0)$  in Fig. 7 exhibit peaks on those parts of the quasi-particle Fermi surfaces which are close to the bare Fermi surface. Some of these parts have the form of Fermi arcs, which, depending on the parameters, can be situated near the nodal directions (near the Brillouin zone diagonal) or in the antinodal region.

Nowhere in the stripe ordered regime we find a simple collection of four nodal Fermi arcs as observed experimentally in the pseudogap regime [60]. Such nodal Fermi arcs are obtained theoretically in a state with fluctuating Néel or spiral magnetic order [16]. Hence, pseudogap behavior with four nodal Fermi arcs must be due to fluctuating Néel or spiral order rather than fluctuating stripe order.

#### IV. CONCLUSIONS

We have presented an  $SU(2)$  gauge theory of fluctuating stripe order in the two-dimensional Hubbard model. Our theory is based on a fractionalization of the electron operators in a fermionic chargon with a pseudospin degree of freedom, and a charge-neutral spinon capturing fluctuations of the spin orientation [18–21]. The chargons are treated in a renormalized mean-field theory with an effective interaction obtained from a renormalization group flow. We have focused on regions in the phase diagram where the chargons order in a spin-charge stripe pattern, which occurs generically at sufficiently large hole-doping [29, 30]. Fluctuations of the spin orientation are described by a nonlinear sigma model. The parameters of the sigma model, the spatial and temporal pseudospin stiffnesses, have been computed from a renormalized RPA. Our approximations are applicable for a moderate Hubbard interaction. The spinon fluctuations prevent breaking of the physical  $SU(2)$  spin symmetry of the Hubbard model at any finite temperature, in agreement with the Mermin-Wagner theorem, resulting in a charge ordered pseudogap phase with a reconstructed Fermi surface and a spin gap.

Concrete solutions have been obtained for a moderate Hubbard interactions  $U = 5t$ . Solving the renormalized mean-field equations we have computed the spin and charge amplitudes defining the stripe profile. The bare dispersion is split into numerous quasi-particle subbands, their number being proportional to the periodicity of the stripe pattern. Correspondingly, the Fermi surface is fragmented into a collection of electron and/or hole pockets and open lines. While the stripe profile (in real space) is never strictly harmonic, it is usually dominated by one Fourier component, that is, a single wave vector. The charge order wave vector and the deviation of the spin order wave vector from  $(\pi, \pi)$  increase monotonically and almost linearly with hole-doping, and only along one of the momentum axes ( $q_x$  or  $q_y$ ).

Small electron pockets have been identified in regions of (fluctuating) charge order of cuprates via quantum oscillation and transport experiments [2]. To obtain such pockets from charge order alone requires a superposition of multiple (non-collinear) ordering wave vectors [61]. Stripe order offers another natural mechanism for electron pockets, where a single (uni-unidirectional) wave vector is sufficient.

Deep inside the stripe regime in the phase diagram, the spatial and temporal pseudospin stiffnesses are of the same order of magnitude as for the Néel state at half-filling. Both

quantities decrease upon approaching the edge of the magnetically ordered region at large hole-doping, and also upon increasing the temperature. In the ground state, the stiffnesses determine the stability of the magnetically ordered mean-field state with respect to quantum fluctuations. Since the ground state of the Hubbard model at half-filling is known to exhibit antiferromagnetic long-range order from (sign-free) Monte Carlo calculations, the sizable stiffnesses in the stripe ordered hole-doped regime indicate that the magnetic order may be robust with respect to fluctuations at  $T = 0$ . Indeed, a stripe ordered ground state has been found for several sizable values of the hole-doping in exact numerical simulations [31–33].

We have computed the spectral function  $A(\mathbf{k}, \omega)$  for single-particle excitations, a quantity that can be measured by angular resolved photoemission [60]. In a normal Fermi liquid,  $A(\mathbf{k}, 0)$  exhibits a pronounced peak at the Fermi surface. In a state with magnetic and/or charge order,  $A(\mathbf{k}, 0)$  is peaked at the (reconstructed) Fermi surface of the quasi-particles. The size of the peaks is strongly momentum dependent due to weight factors which are very small for momenta  $\mathbf{k}$  remote from the bare Fermi surface [22]. The spinon fluctuations broaden the peaks to some extent. Indeed, the spectral function  $A(\mathbf{k}, 0)$  obtained in our theory of fluctuating stripe order exhibits pronounced peaks on those parts of the quasi-particle Fermi surfaces which are close to the bare Fermi surface. Some of these parts have the form of Fermi arcs, but not necessarily centered around the nodal directions (near the Brillouin zone diagonal). Nowhere in the stripe ordered regime we have found a simple collection of four nodal Fermi arcs as observed experimentally in the pseudogap regime [60], and found theoretically in a state with fluctuating Néel or spiral magnetic order [16]. Hence, we conclude that pseudogap behavior with four nodal Fermi arcs must be due to fluctuating Néel or spiral order rather than fluctuating stripe order.

While the spinon fluctuations preserve the physical  $SU(2)$  spin symmetry, at least at finite temperatures, the charge order and nematicity associated with the stripe order of the chargons remains. Commensurate charge order is not excluded by the Mermin-Wagner theorem, as it breaks only a discrete, not a continuous symmetry. Charge order has indeed been observed in some cuprate compounds in the presence of a strong magnetic field, which suppresses the competing superconductivity [62, 63], and the ordering wave vector is oriented along the  $q_x$  or  $q_y$  axes, in agreement with our results.

The treatment of the chargons by renormalized mean-field theory is applicable only for a weak or moderate Hubbard interaction. Our theory can be extended to strong coupling by

computing the chargin order parameter and the corresponding pseudospin stiffnesses from dynamical mean-field theory.

### ACKNOWLEDGEMENTS

We thank Demetrio Vilardi for computing the renormalized Hubbard interaction, and for valuable comments on our manuscript. We are grateful to Andrey Chubukov, Jakob Dolgner, Antoine Georges, Subir Sachdev, Mathias Scheurer, Robin Scholle, Oleg Sushkov, and Hiroyuki Yamase for valuable discussions. P.M.B. acknowledges support by the German National Academy of Sciences Leopoldina through Grant No. LPDS 2023-06 and the Gordon and Betty Moore Foundation's EPiQS Initiative Grant GBMF8683.

### Appendix A: Alternative Ward identity

Another Ward identity holds for a *modified* gauge kernel  $\bar{K}_{\mu\nu}^{ab}$ , which is related to  $K_{\mu\nu}^{ab}$  by a Legendre transform. In Ref. [40] it was assumed that  $\bar{K}_{\mu\nu}^{ab} = K_{\mu\nu}^{ab}$ , but later it was shown that they actually differ [52, 53]. In a magnetic state with an arbitrary spin order  $\langle \mathbf{S}(x) \rangle = \mathbf{m}(\mathbf{r})$ , the modified gauge kernel obeys the Ward identity [40, 53]

$$\partial_\mu \partial'_\nu \bar{K}_{\mu\nu}^{aa'}(x, x') = \epsilon^{abc} \epsilon^{a'b'c'} C^{bb'}(x, x') m^c(\mathbf{r}) m^{c'}(\mathbf{r}'), \quad (\text{A1})$$

where  $C^{bb'}(x, x')$  is the *inverse* spin susceptibility, related to  $\chi^{aa'}(x, x')$  by

$$\int_{x''} C^{aa''}(x, x'') \chi^{a''a'}(x'', x') = \delta_{aa'} \delta(x - x'). \quad (\text{A2})$$

Unlike the Ward identity presented in the main text, this identity does not involve an external symmetry breaking field. For collinear stripe order with a spin profile  $S^1(\mathbf{r})$  in  $x$ -direction, the Ward identity reads

$$\partial_\mu \partial'_\nu \bar{K}_{\mu\nu}^{aa'}(x, x') = \begin{cases} C^{\bar{a}\bar{a}}(x, x') m^1(\mathbf{r}) m^1(\mathbf{r}') & \text{for } a = a' \in \{2, 3\} \\ -C^{\bar{a}\bar{a}'}(x, x') m^1(\mathbf{r}) m^1(\mathbf{r}') & \text{for } a \neq a' \in \{2, 3\} \\ 0 & \text{else} \end{cases}, \quad (\text{A3})$$

with  $\bar{2} = 3$  and  $\bar{3} = 2$ . Defining a *weighted* inverse spin correlation function as

$$\tilde{C}^{aa'}(x, x') = \frac{1}{m^2} m^1(\mathbf{r}) m^1(\mathbf{r}') C^{aa'}(x, x'), \quad (\text{A4})$$

and Fourier transforming, yields

$$(\mathbf{q}, iq_0)_\mu (\mathbf{q}', iq'_0)_\nu \bar{K}_{\mu\nu}^{aa'}(q, q') = \begin{cases} m^2 \tilde{C}^{\bar{a}\bar{a}}(q, q') & \text{for } a = a' \in \{2, 3\} \\ -m^2 \tilde{C}^{\bar{a}\bar{a}'}(q, q') & \text{for } a \neq a' \in \{2, 3\} \\ 0 & \text{else} \end{cases} . \quad (\text{A5})$$

We define modified stiffnesses in analogy to Eq. (13) and (14) as

$$\bar{J}_{\alpha\beta}^{ab} = \lim_{\mathbf{q} \rightarrow 0} \bar{K}_{\alpha\beta}^{ab}(\mathbf{q}, 0), \quad (\text{A6})$$

$$\bar{Z}^{ab} = -\lim_{q_0 \rightarrow 0} \bar{K}_{00}^{ab}(\mathbf{0}, 0), \quad (\text{A7})$$

where  $\bar{K}_{\alpha\beta}^{ab}(q) = \bar{K}_{\alpha\beta}^{ab}(q, q)$ . The Ward identity Eq. (A5) then yields the relations

$$\bar{J}_{\alpha\beta}^{aa} = \frac{m^2}{2} \partial_{q_\alpha} \partial_{q_\beta} \tilde{C}^{\bar{a}\bar{a}}(q, q) \Big|_{q=0}, \quad (\text{A8})$$

$$\bar{Z}^{aa} = \frac{m^2}{2} \partial_{q_0}^2 \tilde{C}^{\bar{a}\bar{a}}(q, q) \Big|_{q=0}. \quad (\text{A9})$$

For a Néel or spiral state, the modified stiffnesses and the stiffnesses defined via  $K_{\mu\nu}^{ab}$  in an infinitesimal external field are actually identical, that is,  $\bar{J}_{\alpha\beta}^{aa} = J_{\alpha\beta}^{aa}$  and  $\bar{Z}^{aa} = Z^{aa}$ , as shown in Refs. [52, 53]. We expect analogous relations to hold in the case of stripe order, too, but refrain from working out a detailed proof, because they are not relevant for our results.

## Appendix B: Cancellation of stiffness contributions

Here we show that the diamagnetic and the bare paramagnetic contributions to the 11-component of the stiffness,  $J_{\alpha\beta}^{11}$ , cancel each other. We start from the expression (58) for the diamagnetic contribution and rewrite it by a partial integration.

$$\begin{aligned} K_{\alpha\beta}^{d,11} &= \frac{T}{4} \sum_{k_0} \int_{\mathbf{k}}' \text{tr} \left[ \Gamma_{\mathbf{k}}^{d,\alpha\beta} \mathcal{G}(k) \right] = \frac{T}{2} \sum_{k_0} \int_{\mathbf{k}}' \text{tr} \left[ (\partial_{k_\beta} \Gamma_{\mathbf{k}}^{\alpha,+} \mathcal{G}_\sigma(k)) \right] \\ &= -\frac{T}{2} \sum_{k_0} \int_{\mathbf{k}}' \text{tr} \left[ \Gamma_{\mathbf{k}}^{\alpha,+} \partial_{k_\beta} (ik_0 - \mathcal{H}_{\mathbf{k}})^{-1} \right] \\ &= \frac{T}{2} \sum_{k_0} \int_{\mathbf{k}}' \text{tr} \left[ \Gamma_{\mathbf{k}}^{\alpha,+} \mathcal{G}_\sigma(k) [\partial_{k_\beta} (ik_0 - \mathcal{H}_{\mathbf{k}})] \mathcal{G}_\sigma(k) \right] \\ &= -\frac{T}{2} \sum_{k_0} \int_{\mathbf{k}}' \text{tr} \left[ \Gamma_{\mathbf{k}}^{\alpha,+} \mathcal{G}_\sigma(k) \Gamma_{\mathbf{k}}^{\beta,+} \mathcal{G}_\sigma(k) \right] = -J_{\alpha\beta,0}^{p,11}. \end{aligned} \quad (\text{B1})$$

Hence,  $K_{\alpha\beta}^{d,11} + J_{\alpha\beta,0}^{p,11} = 0$ .

- 
- [1] B. Keimer, S. A. Kivelson, M. R. Norman, S. Uchida, and J. Zaanen, From quantum matter to high-temperature superconductivity in copper oxides, [Nature](#) **518**, 179 (2015).
  - [2] C. Proust and L. Taillefer, The Remarkable Underlying Ground States of Cuprate Superconductors, [Annu. Rev. Condens. Matter Phys.](#) **10**, 409 (2019).
  - [3] P. W. Anderson, The Resonating Valence Bond State in  $\text{La}_2\text{CuO}_4$  and Superconductivity, [Science](#) **235**, 1196 (1987).
  - [4] F. C. Zhang and T. M. Rice, Effective Hamiltonian for the superconducting Cu oxides, [Phys. Rev. B](#) **37**, 3759 (1988).
  - [5] M. Qin, T. Schäfer, S. Andergassen, P. Corboz, and E. Gull, The Hubbard Model: A Computational Perspective, [Annu. Rev. Condens. Matter Phys.](#) **13**, 275 (2022).
  - [6] O. Gunnarsson, T. Schäfer, J. P. F. LeBlanc, E. Gull, J. Merino, G. Sangiovanni, G. Rohringer, and A. Toschi, Fluctuation Diagnostics of the Electron Self-Energy: Origin of the Pseudogap Physics, [Phys. Rev. Lett.](#) **114**, 236402 (2015).
  - [7] T. Moriya and K. Ueda, Spin fluctuations and high temperature superconductivity, [Adv. Phys.](#) **49**, 555 (2000).
  - [8] Y. M. Vilks and A.-M. S. Tremblay, Destruction of Fermi-liquid quasiparticles in two dimensions by critical fluctuations, [Europhys. Lett.](#) **33**, 159 (1996).
  - [9] P. A. Lee, N. Nagaosa, and X.-G. Wen, Doping a Mott insulator: Physics of high-temperature superconductivity, [Rev. Mod. Phys.](#) **78**, 17 (2006).
  - [10] K.-Y. Yang, T. M. Rice, and F.-C. Zhang, Phenomenological theory of the pseudogap state, [Phys. Rev. B](#) **73**, 174501 (2006).
  - [11] S. Sachdev and D. Chowdhury, The novel metallic states of the cuprates: Topological Fermi liquids and strange metals, [Prog. Theor. Exp. Phys.](#) **2016**, 12C102 (2016).
  - [12] S. Chatterjee, S. Sachdev, and A. Eberlein, Thermal and electrical transport in metals and superconductors across antiferromagnetic and topological quantum transitions, [Phys. Rev. B](#) **96**, 075103 (2017).
  - [13] M. S. Scheurer, S. Chatterjee, W. Wu, M. Ferrero, A. Georges, and S. Sachdev, Topological order in the pseudogap metal, [Proc. Natl. Acad. Sci. USA](#) **115**, E3665 (2018).

- [14] W. Wu, M. S. Scheurer, S. Chatterjee, S. Sachdev, A. Georges, and M. Ferrero, Pseudogap and Fermi-Surface Topology in the Two-Dimensional Hubbard Model, [Phys. Rev. X \*\*8\*\*, 021048 \(2018\)](#).
- [15] S. Sachdev, H. D. Scammell, M. S. Scheurer, and G. Tarnopolsky, Gauge theory for the cuprates near optimal doping, [Phys. Rev. B \*\*99\*\*, 054516 \(2019\)](#).
- [16] P. M. Bonetti and W. Metzner, SU(2) gauge theory of the pseudogap phase in the two-dimensional Hubbard model, [Phys. Rev. B \*\*106\*\*, 205152 \(2022\)](#).
- [17] P. Forni, P. M. Bonetti, H. Müller-Groeling, D. Vilaridi, and W. Metzner, [Spin susceptibility in a pseudogap state with fluctuating spiral magnetic order \(2025\)](#), [arXiv:2509.07826 \[cond-mat.str-el\]](#).
- [18] H. Schulz, Functional Integrals for Correlated Electrons, in *The Hubbard Model*, edited by D. Baeriswyl (Plenum, New York, 1995).
- [19] N. Dupuis, Spin fluctuations and pseudogap in the two-dimensional half-filled Hubbard model at weak coupling, [Phys. Rev. B \*\*65\*\*, 245118 \(2002\)](#).
- [20] K. Borejsza and N. Dupuis, Antiferromagnetism and single-particle properties in the two-dimensional half-filled Hubbard model: A nonlinear sigma model approach, [Phys. Rev. B \*\*69\*\*, 085119 \(2004\)](#).
- [21] S. Sachdev, M. A. Metlitski, Y. Qi, and C. Xu, Fluctuating spin density waves in metals, [Phys. Rev. B \*\*80\*\*, 155129 \(2009\)](#).
- [22] A. Eberlein, W. Metzner, S. Sachdev, and H. Yamase, Fermi surface reconstruction and drop in the hall number due to spiral antiferromagnetism in high- $T_c$  cuprates, [Phys. Rev. Lett. \*\*117\*\*, 187001 \(2016\)](#).
- [23] J. Mitscherling and W. Metzner, Longitudinal conductivity and hall coefficient in two-dimensional metals with spiral magnetic order, [Phys. Rev. B \*\*98\*\*, 195126 \(2018\)](#).
- [24] P. M. Bonetti, J. Mitscherling, D. Vilaridi, and W. Metzner, Charge carrier drop at the onset of pseudogap behavior in the two-dimensional Hubbard model, [Phys. Rev. B \*\*101\*\*, 165142 \(2020\)](#).
- [25] Y.-H. Zhang and S. Sachdev, From the pseudogap metal to the Fermi liquid using ancilla qubits, [Phys. Rev. Res. \*\*2\*\*, 023172 \(2020\)](#).
- [26] Y.-H. Zhang and S. Sachdev, Deconfined criticality and ghost Fermi surfaces at the onset of antiferromagnetism in a metal, [Phys. Rev. B \*\*102\*\*, 155124 \(2020\)](#).

- [27] E. Mascot, A. Nikolaenko, M. Tikhanovskaya, Y.-H. Zhang, D. K. Morr, and S. Sachdev, Electronic spectra with paramagnon fractionalization in the single-band Hubbard model, [Phys. Rev. B \*\*105\*\*, 075146 \(2022\)](#).
- [28] A. Nikolaenko, J. von Milczewski, D. G. Joshi, and S. Sachdev, Spin density wave, Fermi liquid, and fractionalized phases in a theory of antiferromagnetic metals using paramagnons and bosonic spinons, [Phys. Rev. B \*\*108\*\*, 045123 \(2023\)](#).
- [29] R. Scholle, P. M. Bonetti, D. Vilardi, and W. Metzner, Comprehensive mean-field analysis of magnetic and charge orders in the two-dimensional Hubbard model, [Phys. Rev. B \*\*108\*\*, 035139 \(2023\)](#).
- [30] R. Scholle, W. Metzner, D. Vilardi, and P. M. Bonetti, Spiral to stripe transition in the two-dimensional Hubbard model, [Phys. Rev. B \*\*109\*\*, 235149 \(2024\)](#).
- [31] B.-X. Zheng, C.-M. Chung, P. Corboz, G. Ehlers, M.-P. Qin, R. M. Noack, H. Shi, S. R. White, S. Zhang, and G. K.-L. Chan, Stripe order in the underdoped region of the two-dimensional Hubbard model, [Science \*\*358\*\*, 1155 \(2017\)](#).
- [32] E. W. Huang, C. B. Mendl, H.-C. Jiang, B. Moritz, and T. P. Devereaux, Stripe order from the perspective of the Hubbard model, [npj Quantum Mater. \*\*3\*\*, 22 \(2018\)](#).
- [33] M. Qin, C.-M. Chung, H. Shi, E. Vitali, C. Hubig, U. Schollwöck, S. R. White, and S. Zhang (Simons Collaboration on the Many-Electron Problem), Absence of Superconductivity in the Pure Two-Dimensional Hubbard Model, [Phys. Rev. X \*\*10\*\*, 031016 \(2020\)](#).
- [34] H. Xu, H. Shi, E. Vitali, M. Qin, and S. Zhang, Stripes and spin-density waves in the doped two-dimensional Hubbard model: Ground state phase diagram, [Phys. Rev. Res. \*\*4\*\*, 013239 \(2022\)](#).
- [35] H. Xu, C.-M. Chung, M. Qin, U. Schollwöck, S. R. White, and S. Zhang, Coexistence of superconductivity with partially filled stripes in the Hubbard model, [Science \*\*384\*\*, eadh7691 \(2024\)](#).
- [36] H. Schlömer, A. Bohrdt, and F. Grusdt, Geometric Orthogonal Metals: Hidden Antiferromagnetism and the Pseudogap from Fluctuating Stripes, [PRX Quantum \*\*6\*\*, 030342 \(2025\)](#).
- [37] X. Zhang and N. Bultinck, [Strange metal and Fermi arcs from disordering spin stripes \(2025\)](#), [arXiv:2507.06309 \[cond-mat.str-el\]](#).
- [38] D. P. Arovas, E. Berg, S. A. Kivelson, and S. Raghu, The Hubbard Model, [Annu. Rev. Condens. Matter Phys. \*\*13\*\*, 239 \(2022\)](#).

- [39] J. W. Negele and H. Orland, *Quantum Many-Particle Systems* (Addison-Wesley, Reading, 1987).
- [40] P. M. Bonetti, Local Ward identities for collective excitations in fermionic systems with spontaneously broken symmetries, *Phys. Rev. B* **106**, 155105 (2022).
- [41] A. Auerbach, *Interacting Electrons and Quantum Magnetism* (Springer-Verlag, New York, 1994).
- [42] J. Wang, A. Eberlein, and W. Metzner, Competing order in correlated electron systems made simple: Consistent fusion of functional renormalization and mean-field theory, *Phys. Rev. B* **89**, 121116 (2014).
- [43] W. Metzner, M. Salmhofer, C. Honerkamp, V. Meden, and K. Schönhammer, Functional renormalization group approach to correlated fermion systems, *Rev. Mod. Phys.* **84**, 299 (2012).
- [44] H. Yamase, A. Eberlein, and W. Metzner, Coexistence of Incommensurate Magnetism and Superconductivity in the two-dimensional Hubbard Model, *Phys. Rev. Lett.* **116**, 096402 (2016).
- [45] D. Vilaridi, P. M. Bonetti, and W. Metzner, Dynamical functional renormalization group computation of order parameters and critical temperatures in the two-dimensional Hubbard model, *Phys. Rev. B* **102**, 245128 (2020).
- [46] J. Zaanen and O. Gunnarsson, Charged magnetic domain lines and the magnetism of high- $T_c$  oxides, *Phys. Rev. B* **40**, 7391 (1989).
- [47] H. J. Schulz, Domain walls in a doped antiferromagnet, *J. Phys. France* **50**, 2833 (1989).
- [48] K. Machida, Magnetism in  $\text{La}_2\text{CuO}_4$  based compounds, *Physica C: Superconductivity* **158**, 192 (1989).
- [49] D. Poilblanc and T. M. Rice, Charged solitons in the Hartree-Fock approximation to the large- $U$  Hubbard model, *Phys. Rev. B* **39**, 9749 (1989).
- [50] H. J. Schulz, Incommensurate antiferromagnetism in the two-dimensional Hubbard model, *Phys. Rev. Lett.* **64**, 1445 (1990).
- [51] M. Kato, K. Machida, H. Nakanishi, and M. Fujita, Soliton Lattice Modulation of Incommensurate Spin Density Wave in Two Dimensional Hubbard Model -A Mean Field Study, *J. Phys. Soc. Jpn.* **59**, 1047 (1990).
- [52] P. M. Bonetti, Erratum: Local Ward identities for collective excitations in fermionic systems with spontaneously broken symmetries [Phys. Rev. B 106, 155105 (2022)], *Phys. Rev. B* **110**, 079902 (2024).

- [53] I. A. Goremykin and A. A. Katanin, Antiferromagnetic and spin spiral correlations in the doped two-dimensional Hubbard model: Gauge symmetry, Ward identities, and dynamical mean-field theory analysis, [Phys. Rev. B \*\*110\*\*, 085153 \(2024\)](#).
- [54] G. Baym and L. P. Kadanoff, Conservation Laws and Correlation Functions, [Phys. Rev. \*\*124\*\*, 287 \(1961\)](#).
- [55] R. Penrose, A generalized inverse for matrices, [Mathematical Proceedings of the Cambridge Philosophical Society \*\*51\*\*, 406 \(1955\)](#).
- [56] S. Sachdev, A. V. Chubukov, and A. Sokol, Crossover and scaling in a nearly antiferromagnetic Fermi liquid in two dimensions, [Phys. Rev. B \*\*51\*\*, 14874 \(1995\)](#).
- [57] E. Pavarini, I. Dasgupta, T. Saha-Dasgupta, O. Jepsen, and O. K. Andersen, Band-Structure Trend in Hole-Doped Cuprates and Correlation with  $T_{c\max}$ , [Phys. Rev. Lett. \*\*87\*\*, 047003 \(2001\)](#).
- [58] P. M. Bonetti and W. Metzner, Spin stiffness, spectral weight, and Landau damping of magnons in metallic spiral magnets, [Phys. Rev. B \*\*105\*\*, 134426 \(2022\)](#).
- [59] D. Vilardi, P. M. Bonetti, and W. Metzner, Spin stiffnesses and stability of magnetic order in the lightly doped two-dimensional Hubbard model, [Phys. Rev. B \*\*112\*\*, 245149 \(2025\)](#).
- [60] A. Damascelli, Z. Hussain, and Z.-X. Shen, Angle-resolved photoemission studies of the cuprate superconductors, [Rev. Mod. Phys. \*\*75\*\*, 473 \(2003\)](#).
- [61] N. Harrison and S. E. Sebastian, Protected Nodal Electron Pocket from Multiple- $\mathbf{Q}$  Ordering in Underdoped High Temperature Superconductors, [Phys. Rev. Lett. \*\*106\*\*, 226402 \(2011\)](#).
- [62] T. Wu, H. Mayaffre, S. Krämer, M. Horvatić, C. Berthier, W. N. Hardy, R. Liang, D. A. Bonn, and M.-H. Julien, Magnetic-field-induced charge-stripe order in the high-temperature superconductor  $\text{YBa}_2\text{Cu}_3\text{O}_y$ , [Nature \*\*477\*\*, 191 \(2011\)](#).
- [63] J. Chang, E. Blackburn, A. T. Holmes, N. B. Christensen, J. Larsen, J. Mesot, R. Liang, D. A. Bonn, W. N. Hardy, A. Watenphul, M. v. Zimmermann, E. M. Forgan, and S. M. Hayden, Direct observation of competition between superconductivity and charge density wave order in  $\text{YBa}_2\text{Cu}_3\text{O}_{6.67}$ , [Nature Physics \*\*8\*\*, 871 \(2012\)](#).